Journal of Medicinal Chemistry

Article

pubs.acs.org/jmc

# Structural Optimization of Quinolon-4(1*H*)-imines as Dual-Stage Antimalarials: Toward Increased Potency and Metabolic Stability

Ana S. Ressurreição,*[,†,∞] Daniel Gonçalves,[†,∞] Ana R. Sitoe,[†] Inês S. Albuquerque,[‡] Jiri Gut,[∥] Ana Góis,[‡] Lídia M. Gonçalves,[†] Maria R. Bronze,[†] Thomas Hanscheid,[‡] Giancarlo A. Biagini,[⊥] Philip J. Rosenthal,[∥] Miguel Prudêncio,[‡] Paul O'Neill,[#] Maria M. Mota,[‡] Francisca Lopes,[†] and Rui Moreira[†]

[†]Research Institute for Medicines and Pharmaceutical Sciences (iMed.UL), Faculty of Pharmacy, University of Lisbon, Av. Prof. Gama Pinto, 1649-019 Lisbon, Portugal

[‡]Instituto de Medicina Molecular, Faculty of Medicine, University of Lisbon, Av. Prof. Egas Moniz, 1649-028 Lisbon, Portugal

[∥]Department of Medicine, San Francisco General Hospital, University of California, Box 0811, San Francisco, California 94143, United States

[⊥]Liverpool School of Tropical Medicine, Pembroke Place, Liverpool, L3 5QA, U.K.

[#]Department of Chemistry, University of Liverpool, Liverpool, L69 3BX, U.K.

Supporting Information

**ABSTRACT:** Discovery of novel effective and safe antimalarials has been traditionally focused on targeting erythrocytic parasite stages that cause clinical symptoms. However, elimination of malaria parasites from the human population will be facilitated by intervention at different life-cycle stages of the parasite, including the obligatory developmental phase in the liver, which precedes the erythrocytic stage. We have previously reported that *N*-Mannich-based quinolon-4(1*H*)-imines are potent antiplasmodial agents but present several stability liabilities. We now report our efforts to optimize quinolon-4(1*H*)-imines as dual-stage antiplasmodial agents endowed with chemical and metabolic stability. We report compounds active against both the erythrocytic and exoerythrocytic forms of malaria parasites, such as the quinolon-4(1*H*)-imine **5p** ($IC_{50}$ values of 54 and 710 nM against the erythrocytic and exoerythrocytic forms), which constitute excellent starting points for further lead optimization as dual-stage antimalarials.

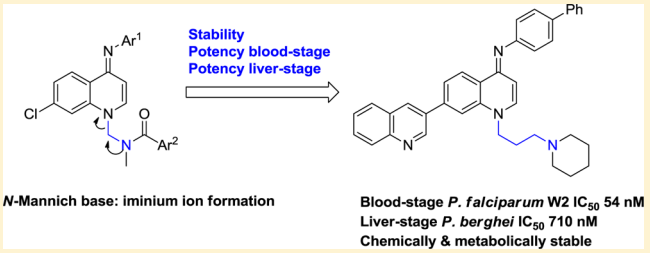


## INTRODUCTION

Malaria remains a major global public health problem, affecting over 200 million people mainly in tropical and subtropical regions and with an estimated death toll of nearly 800 000 individuals in 2011.[1,2] Five species from the genus *Plasmodium* cause infection in humans. Of these, *P. falciparum* and *P. vivax* account for more than 95% of malaria cases, with *P. falciparum* responsible for most of the deaths caused by malaria every year. The rapid evolution and spread of parasite resistance to most available antimalarial drugs threaten the use of these agents to treat and prevent malaria.[3,4] To address the need for new and safe drugs for treating or preventing malaria, large phenotypic high-throughput screening campaigns[5,6] have been performed to discover novel chemotypes acting against erythrocytic stage parasites, which are responsible for the clinical features of malaria. However, global control and eventual eradication of malaria will benefit from action against multiple parasite life-cycle stages.[7,8]

Malaria parasites undergo an asymptomatic, obligatory developmental phase in the liver, which precedes the formation of the erythrocytic stage.[9] In addition, *P. vivax* and *P. ovale* infections also generate liver forms, called hypnozoites, that are not eliminated by standard therapy, persist in the liver for long periods, and upon reactivation, are responsible for relapses of malaria.[10] Thus, the liver stage of infection offers an important target for intervention in addition to erythrocytic stages. Indeed, eradication of liver-stage parasites can provide causal prophylaxis, with elimination of parasites before the development of symptomatic infection.[11] Drugs active against hypnozoites will also facilitate malaria elimination campaigns.[10,12] Primaquine (**1**, Figure 1), an 8-aminoquinoline (8-AQ), acts against liver forms of all *Plasmodium* species and is the only available antimalarial that acts against *P. vivax* and *P. ovale* hypnozoites, thereby preventing relapses after treatment for malaria. However, primaquine has significant side effects, including hemolysis in patients with glucose 6-phosphate dehydrogenase deficiency, a common genetic abnormality in malaria-endemic regions.[13] The liver stage of infection has been underexploited as an antimalarial target because of the poorly understood biology of *Plasmodium* liver stages and technical difficulties in studying them.[11,14] Only recently have systematic

**Received:** July 28, 2013
**Published:** September 10, 2013

  

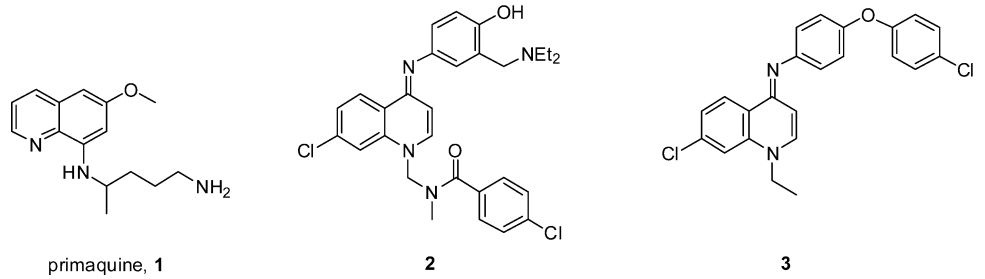


**Figure 1.** Structures of primaquine (**1**), a *N*-Mannich-based quinolon-4(1*H*)-imine (**2**), and a *N*-alkyl-quinolon-4-(1*H*)-imine (**3**).

**Scheme 1. Mechanism for the Acid-Catalyzed Hydrolysis of *N*-Mannich-Based Quinolon-4(1*H*)-imine, 2**

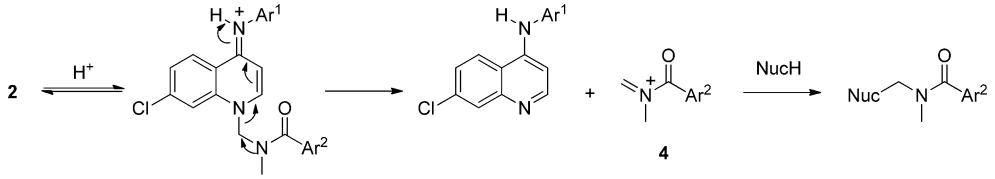


efforts toward the identification of novel scaffolds active against *Plasmodium* liver stages, including phenotypic approaches, resulted in the discovery of potent compounds.[15−17]

We previously reported that *N*-Mannich-based quinolon-4(1*H*)-imines derived from amodiaquine (e.g., **2**, Figure 1) are potent antiplasmodial agents, with low nanomolar $IC_{50}$ values against the chloroquine-resistant *P. falciparum* Dd2 strain.[18] Quinolon-4(1*H*)-imines **2** were shown to hydrolyze to amodiaquine in aqueous solutions, particularly at low pH values, thus raising the possibility of these compounds acting as chemically activated prodrugs. The mechanism of hydrolysis probably involves protonation of the 4-imino nitrogen atom, followed by alkyl C−N bond scission via an $S_N1$ mechanism, leading to the formation of amodiaquine and the corresponding secondary amide (Scheme 1).[18] This mechanism is similar to that reported for the acid-catalyzed hydrolysis of *N*-acyloxymethyl[19−21] and *N*-amidomethyl prodrugs[22] and involves the formation of an iminium ion intermediate, **4**, which can alkylate biomolecules, potentially contributing to toxicity.[23] More recently, we have disclosed a library of *N*-alkyl-quinolon-4(1*H*)-imines (e.g., **3**, Figure 1), lacking the *N*-Mannich base moiety, as potent antiplasmodial agents that target the liver stage of infection.[24] However, these compounds were shown to be degraded in rat liver microsomes with half-lives of ∼4 h. We now report our strategy to improve stability toward aqueous buffers and microsomal enzymes by introducing an aminoalkyl side chain at the N-1 position while simultaneously exploiting the quinolon-4(1*H*)-imine scaffold to optimize antiplasmodial activity (**5**, Figure 2). The studies herein presented led to the discovery of dual-acting analogues active against both blood and liver stages of parasites that are chemically and metabolically stable and lack apparent cytotoxicity.

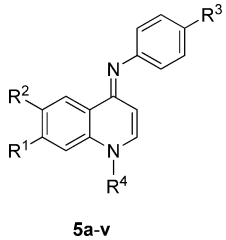


**Figure 2.** General structure for quinolon-4(1*H*)-imines **5** reported in this study. See Table 1 for structures **5a−v**.

## RESULTS AND DISCUSSION

**Chemistry.** The general synthetic approach to quinolon-4(1*H*)-imines **5a−p** is presented in Scheme 2. Briefly, 4-

**Scheme 2. Synthesis of Quinolon-4(1*H*)-imines 5a−p[a]**

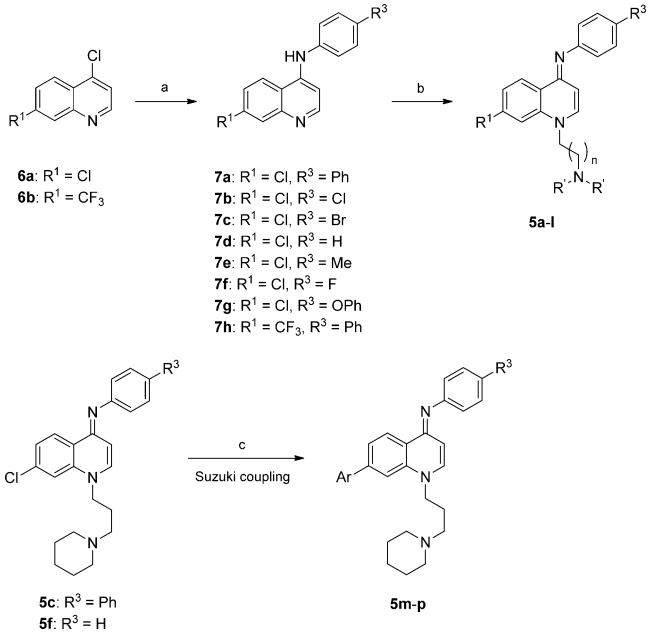


[a]Reagents and conditions: (a) $R^3PhNH_2$, TEA, MeOH, rt, 24 h; (b) chloroalkylamine, NaH, DMF, rt, 5−12 h; (c) $PdCl_2(Ph_3P)_2$, *t*-Bu-Xphos, $Na_2CO_3$ 1 M, boronic acid, dioxane, 100 °C, o/n.

chloroquinolines **6a** and **6b** were reacted with the appropriate anilines in methanol and triethylamine to form the corresponding 4-anilinoquinolines **7a−h** in very good to excellent yields. Intermediates **7** were subsequently transformed into the target compounds **5a−l** in moderate to good yields by reaction with the appropriate chloroalkylamines in DMF in the presence of sodium hydride. X-ray analysis of compound **5c** confirmed that the stereochemistry of the C═N bond corresponds to the *E*


dx.doi.org/10.1021/jm4011466 | J. Med. Chem. 2013, 56, 7679−7690

isomer, in line with other reports.[25] Compounds **5m−p** were prepared from quinolon-4(1*H*)-imines **5c** and **5f** using Suzuki coupling with the appropriate boronic acids or pinacolyl esters. Surprisingly, the product isolated from the reaction of **5c** with 2-aminopyridine-5-boronic acid pinacol ester matches the C−N coupling product **5o**, as confirmed by mono- and bidimensional NMR analysis (see Supporting Information for NMR spectra and complete peak assignment).

Synthesis of compounds **5q−t** required alkylation of intermediates **7a** and **7h** with 1,3-dibromopropane or 1,4-dibromobutane to give the corresponding bromoalkyl-quinolon-4(1*H*)-imines **8a−d**, which were subsequently converted into the compounds **5q−t** by reaction with diethylamine in dichloromethane (Scheme 3). The route to 6-substituted

**Scheme 3. Synthesis of Quinolon-4(1*H*)-imines 5q−t**[a]

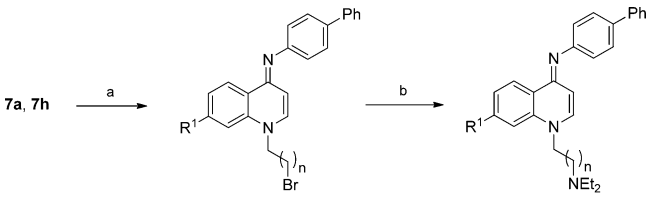


[a]Reagents and conditions: (a) $Br(CH_2)_3Br$ or $Br(CH_2)_4Br$, NaH, DMF, rt, 5 h; (b) $Et_2NH$, THF, rt, o/n.

quinolon-4(1*H*)-imines **5u** and **5v** began with the synthesis of quinolines **6c** and **6d**, following reported procedures.[26,27] Briefly, Gould−Jacobs protocol was applied to the appropriate anilines to form the 6-substituted quinolones **10a** and **10b** (Scheme 4). Hydrolysis of the ethyl ester followed by decarboxylation afforded their analogues **11a** and **11b**, which were converted into the corresponding 4-chloroquinolines by reaction with $POCl_3$. Reaction of **6c** and **6d** with the appropriate aniline followed by alkylation and reduction (as described before) provided the quinolon-4-(1*H*)-imines **5u** and **5v** in good yields.

**Activity against the Erythrocytic Stage of Infection and Cytotoxicity.** Compounds **5a−v** were screened for activity against the erythrocytic stage of chloroquine-resistant *P. falciparum* W2 infection and for cytotoxicity against HEK293T mammalian cells (Table 1). Quinolon-4(1*H*)-imines **5** inhibited the growth of parasites with $IC_{50}$ values ranging from 50 to 520 nM while displaying negligible cytotoxicity, with $EC_{50}$ values against cultured mammalian cells ranging from 7 to ≥100 μM. This result indicates that the quinolon-4(1*H*)-imine scaffold, when attached to an alkylamino side chain through the N-1 nitrogen atom, provides potent antiplasmodial compounds comparable in potency to their *N*-Mannich-base counterparts, **2**,[18] and are approximately 10-fold more potent than the previously reported *N*-alkyl analogues, **3** ($IC_{50}$ values ranging from 0.54 to 5.88 μM).[24] In general, most of the compounds **5a−v** presented selectivity indices (SI = $EC_{50}$(HEK293T)/$IC_{50}$(W2)) higher than 300, indicating that quinolon-4(1*H*)-imines are selective and nontoxic.

Inspection of the activity data against erythrocytic *P. falciparum* presented in Table 1 reveals that compounds with propyl or butyl linkers between the N-1 nitrogen atom of the quinolon-4(1*H*)-imine and the distal acyclic basic moiety are significantly more potent than those with the ethyl linker (e.g., **5q**, **5r** vs **5a**, and **5s**, **5t** vs **5j**). This difference is not observed for compounds containing a distal cyclic basic moiety (e.g., **5b** and **5c**). However, a reasonable correlation ($R^2$ = 0.76) was observed between the $pIC_{50}$ values for the 7-chloro and 7-trifluoromethyl series, suggesting that both series present similar structural requirements regarding the alkylamino side chain at the N-1 nitrogen (Figure 3).

The effect of the electronic and hydrophobic properties of substituents in the quinolon-4(1*H*)-imine scaffold in the activity data in Table 1 was analyzed using the Hansch QSAR method. A good correlation ($R^2$ = 0.82) was found between the $pIC_{50}$ values and the Hansch π values for the substituents at the imine moiety, indicating that more lipophilic substituents improve activity against blood-stage parasites (Figure 4). In contrast, the electronic properties of the

**Scheme 4. Synthesis of Quinolon-4(1*H*)-imines 5u and 5v**[a]

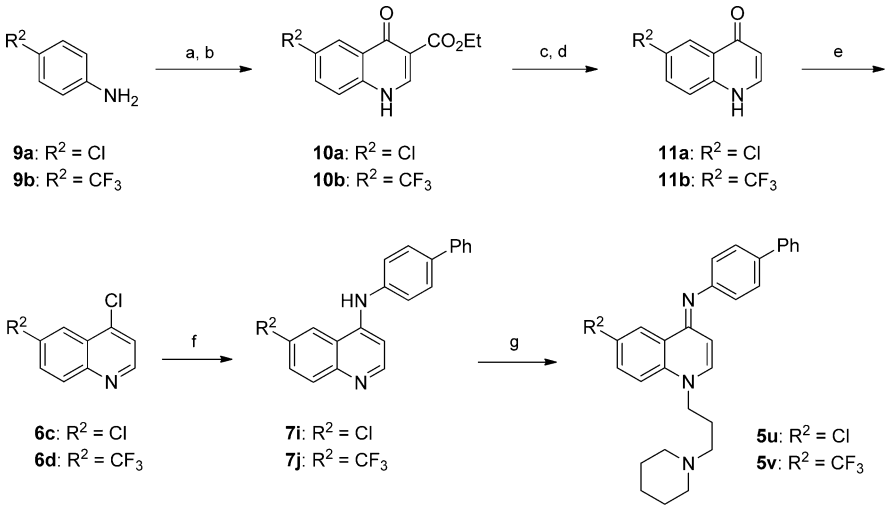


[a]Reagents and conditions: (a) (2-ethoxymethylene)malonate, 110 °C, 2 h; (b) $Ph_2O$, reflux, 1 h; (c) NaOH 2 M, MeOH, reflux, 18 h; (d) $Ph_2O$, reflux, 1 h; (e) $POCl_3$, 140 °C, 4 h; (f) 4-aminobiphenyl, TEA, MeOH, rt, 24 h; (g) 1-(3-chloropropyl)piperidine, NaH, DMF, rt, 12 h.


dx.doi.org/10.1021/jm4011466 | J. Med. Chem. 2013, 56, 7679−7690

**Table 1. Antiplasmodial Activity of Quinolon-4(1*H*)-imines 5a–v and 3 against Blood and Liver Stages of Infection (*P. falciparum* W2 and *P. berghei*, respectively) and Their Cytotoxicity against Human Embryonic Kidney HEK293T Cells**

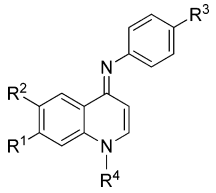


| Compd | $R^1$ | $R^2$ | $R^3$ | $R^4$ | $IC_{50}$ (nM) | | $EC_{50}$ (μM) | SI |
|---|---|---|---|---|---|---|---|---|
| | | | | | Blood-stage | Liver-stage | HEK293T | |
| **5a** | Cl | H | Ph |  | 498 | ND | 37.1 | 74 |
| **5b** | Cl | H | Ph |  | 111 | 3460 | >100 | >900 |
| **5c** | Cl | H | Ph |  | 144 | ND | 41.8 | 290 |
| **5d** | Cl | H | Cl |  | 259 | 2696 | >100 | >386 |
| **5e** | Cl | H | Br |  | 74.0 | 3010 | >100 | >1351 |
| **5f** | Cl | H | H |  | 273 | ND | >100 | >366 |
| **5g** | Cl | H | Me |  | 331 | ND | >100 | >302 |
| **5h** | Cl | H | F |  | 369 | 4783 | >100 | >271 |
| **5i** | Cl | H | OPh |  | 160 | ND | 30.6 | 191 |
| **5j** | $CF_3$ | H | Ph |  | 525 | 4614 | 38.5 | 73 |
| **5k** | $CF_3$ | H | Ph |  | 226 | ND | >100 | >442 |
| **5l** | $CF_3$ | H | Ph |  | 360 | ND | 56.8 | 158 |
| **5m** |  | H | H |  | 216 | 1385 | >100 | >463 |
| **5n** |  | H | Ph |  | 55.4 | 2070 | 7.63 | 138 |
| **5o** |  | H | Ph |  | 357 | 440 | 7.34 | 21 |
| **5p** |  | H | Ph |  | 53.7 | 710 | 7.68 | 143 |
| **5q** | Cl | H | Ph |  | 151 | ND | >100 | >662 |
| **5r** | Cl | H | Ph |  | 67.6 | 2653 | >100 | >1479 |
| **5s** | $CF_3$ | H | Ph |  | 144 | ND | >100 | >694 |
| **5t** | $CF_3$ | H | Ph |  | 50.3 | ND | >100 | >1988 |
| **5u** | H | Cl | Ph |  | 99.7 | ND | 21.8 | 219 |
| **5v** | H | $CF_3$ | Ph |  | 631 | ND | 23.7 | 38 |
| **3** | | | | | 1090[a] | 87.0[a] | -- | -- |
| **CQ** | | | | | 186 | ND | ND | -- |
| **PQ** | | | | | ND | 7500[16] | ND | -- |

[a]From ref 24. ND: not determined; compounds not active at 1 μM. SI: selectivity index = $EC_{50}$(HEK293T)/$IC_{50}$(W2)).


dx.doi.org/10.1021/jm4011466 | *J. Med. Chem.* 2013, 56, 7679–7690

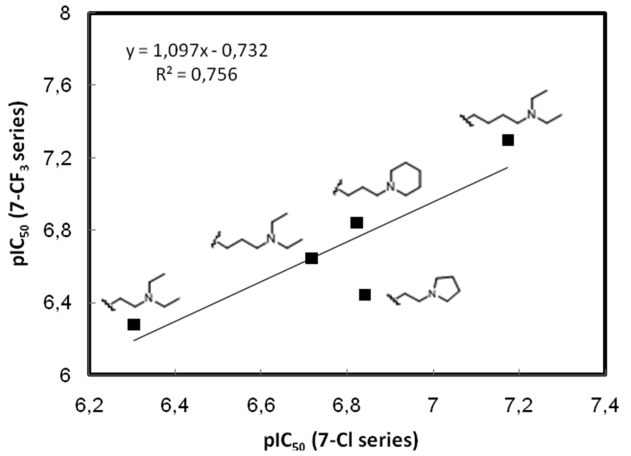


**Figure 3.** Plot of $pIC_{50}$ against *P. falciparum* W2 for the 7-$CF_3$ series (**5j−l,s,t**) versus $pIC_{50}$ for the 7-Cl series (**5a−c,q,r**). The data are from Table 1

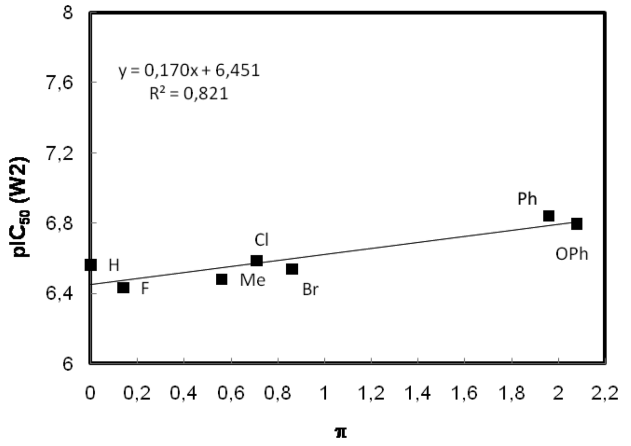


**Figure 4.** Plot of the $pIC_{50}$ of the quinolon-4(1*H*)-imines **5c−i** (*P. falciparum* W2 strain) versus the Hansch $\pi$ values of the substituents in para-position of their phenylimine moiety.

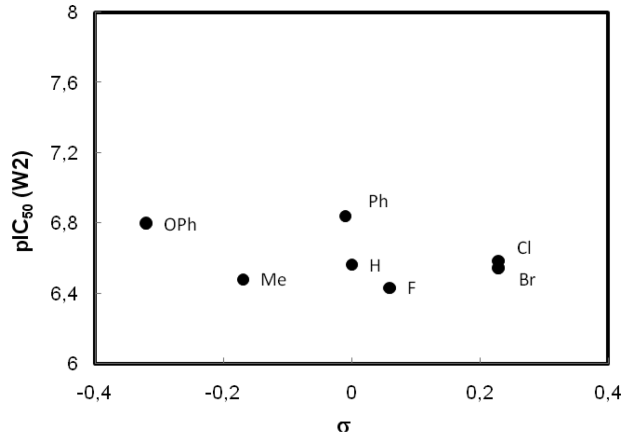


**Figure 5.** Plot of the $pIC_{50}$ of the quinolon-4(1*H*)-imines **5c−i** (*P. falciparum* W2 strain) versus the Hammett $\sigma$ values[28] of the substituents in para-position of their phenylimine moiety.

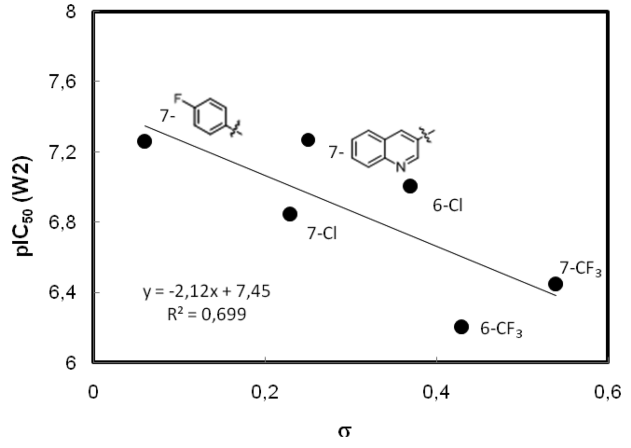


**Figure 6.** Plot of the $pIC_{50}$ of the quinolon-4(1*H*)-imines **5c−i** (*P. falciparum* W2 strain) versus the Hammett $\sigma$ values[28] for substituents in positions C-6 and C-7 of the quinolonimine moiety.

substituents at the imine moiety do not affect the antiplasmodial activity (Figure 5). A moderate correlation ($R^2$ = 0.70) was observed between the $pIC_{50}$ values and the Hammett $\sigma$ values[28] for substituents in positions C-6 and C-7 of the quinolonimine moiety. Selection of Hammett constants was defined relative to the imine function, and thus, $\sigma_{para}$ values were used for substituents at C-7 while $\sigma_{meta}$ values were used for substituents at C-6. As shown in Figure 6, electron-withdrawing substituents at C-6 and C-7 are detrimental to activity of quinolon-4(1*H*)-imines against erythrocytic parasites. This effect probably reflects a decrease in the basicity of the quinolon-4(1*H*)-imine, which can be considered as a vinylogous cyclic amidine[29] with subsequent reduction of accumulation in the acidic digestive vacuole (DV) of the parasite, the site of action of aminoquinoline antimalarials. There is strong evidence that pH trapping plays a role in the activity of aminoquinoline antimalarials such as chloroquine.[30] Interestingly, derivative **5o**, which contains a 2-pyridylamine substituent at C-7, is equipotent to its 7-$CF_3$ counterpart **5l**, a result that might be ascribed to the protonation of the pyridine nitrogen atom within the parasite DV. The protonated 2-pyridylamine is most likely a strong electron-withdrawing substituent, as suggested by the apparent $\sigma_{ortho}$ value of 3.21 for the $=NH^+$ moiety (compared to the value of 0.56 for =N group).[29]

**Inhibition of Heme Polymerization.** *Plasmodium* parasites dispose the free, toxic ferriprotoporphyrin IX (FP) that results from digestion of host erythrocyte hemoglobin by crystallizing it into insoluble hemozoin crystals.[31,32] Recent studies provided robust evidence that chloroquine and other quinoline antimalarials inhibit hemozoin formation by binding to free FP or to the surface of the growing hemozoin crystal.[33,34] Since compounds **5** display a quinoline-related scaffold and two basic sites (the $pK_a$ values for the quinolon-4(1*H*)-imine and distal amine groups are approximately 6−7 and 8−9, respectively[35]), which might lead to accumulation in the acidic DV, we investigated whether they could also inhibit hemozoin formation. Selected quinolon-4(1*H*)-imines **5** were screened using a novel, simple, and efficient in vitro method based on the formation of hemozoin-like crystals.[36] The data presented in Table 2 reveal that the tested compounds **5** are either inactive or poor inhibitors of hemozoin formation when


dx.doi.org/10.1021/jm4011466 | *J. Med. Chem.* 2013, 56, 7679−7690

**Table 2. Inhibition of Hemozoin-like Crystal Formation by Selected Quinolon-4(1*H*)-imines 5 (Middle Column), Chloroquine and Gentamicin (Negative Control), and Comparison to $IC_{50}$ Values on Erythrocytic Stage (Right Column)[a]**

| compd | MIC ($\mu$M) | $IC_{50}$(W2) (nM) |
|---|---|---|
| **5d** | NI[b] | 259 |
| **5f** | NI[b] | 273 |
| **5h** | NI[b] | 369 |
| **5i** | 500 | 160 |
| **5j** | NI[b] | 525 |
| **5k** | NI[b] | 226 |
| **5n** | 500 | 55.4 |
| **5u** | 1000 | 99.7 |
| **5v** | 1000 | 631 |
| chloroquine | 125 | 186 |
| gentamicin | NI[b] | ND[c] |

[a]The inhibition of hemozoin-like crystals formation was tested in the presence of 0−1000 $\mu$M of each compound. [b]NI: no inhibition of hemozoin-like crystal formation. [c]ND: not determined.

compared to chloroquine, thus indicating that this is not the main mechanism of action of **5** against erythrocytic parasites.

**Activity against the Mitochondrial Electron Transport Chain.** Quinolon-4(1*H*)-imines **5** are structurally related to dihydroacridinedione **12** (WR 243251, Figure 7), a potent blood schizonticidal agent.[37,38] Mechanistic studies suggested that dihydroacridinedione **12** targets the parasite mitochondrial electron transport chain (mtETC),[39] which is responsible for maintaining a constant pool of ubiquinone for the last step of pyrimidine biosynthesis, catalyzed by dihydroorotate dehydrogenase (DHODH).[40] The ketone hydrolysis product, a potential metabolite of **12**, appeared to target the $Q_o$ quinol oxidation site of the cytochrome $bc_1$ complex, an essential component of the mtETC.[41] A similar mode of action has been reported for the closely related class of antiplasmodial 4(1*H*)-quinolones[16,42,43] and 4(1*H*)-pyridones[44] (e.g., **13** and **14**, respectively). In order to investigate whether the antiplasmodial mode of action of quinolon-4(1*H*)-imines involved inhibition of the parasite's $bc_1$ complex, we screened compounds **5b**, **5c**, **5l**, and **5r** using a phenotypic assay based on a *P. falciparum* 3D7 cell line transfected with yeast DHODH.[45] This cell line, which uses fumarate instead of ubiquinone as the final electron acceptor, has been shown previously to be resistant to mtETC inhibitors.[46] The results presented in Table 3 indicate that **5b**, **5c**, **5l**, and **5r** display similar antiplasmodial activity against both 3D7-yDHODH and parental 3D7 strains, suggesting that inhibition of the $bc_1$ complex is not the primary antimalarial mode of action for quinolon-4(1*H*)-imines **5**. This result was further supported by the observation that compound **5r** did not inhibit $bc_1$ complex activity at ≤10 $\mu$M (measured as ubiquinol/cytc reductase), from *P. falciparum* cell-free extracts.

**Table 3. Growth Inhibition of Parental (3D7) and Transgenic (3D7-yDHODH) *P. falciparum* Strains with Quinolon-4(1*H*)-imines 5b, 5c, 5l, and 5r**

| | $IC_{50}$ ± SD (nM) | | | |
|---|---|---|---|---|
| *P. falciparum* strain | **5b** | **5c** | **5l** | **5r** |
| 3D7 | 177 ± 14 | 73.7 ± 2.9 | 136 ± 19 | 64.7 ± 1.9 |
| 3D7-yDHODH | 186 ± 42 | 52.3 ± 3.5 | 195 ± 82 | 68.3 ± 1.7 |

**Activity against the Liver Stage of Infection.** Quinolon-4(1*H*)-imines **5** were also evaluated for their antiplasmodial activity against liver stages of the rodent parasite *P. berghei* and for cytotoxicity to Huh-7 human hepatoma cells, employing methods that were previously reported.[47] Primaquine was also included (1 and 10 $\mu$M) as a positive control for liver stage activity. Remarkably, nine compounds were more potent than primaquine and were nontoxic to Huh-7 human hepatoma cells at concentrations up to 5 $\mu$M. These compounds were then submitted to a dose−effect study, and the resulting $IC_{50}$ values for the inhibition of hepatic *P. berghei* infection ranged from 0.44 to 4.6 $\mu$M, which compare favorably with the $IC_{50}$ value of 7.5 $\mu$M determined for primaquine (Table 1). Notably, the most active compounds **5o** and **5p** ($IC_{50}$ values of 0.44 and 0.71 $\mu$M, respectively), which have heterocyclic moieties in position C-7 of the quinolonimine scaffold, were at least 10-fold more potent than primaquine, establishing these novel quinolinimine derivatives as promising dual-stage antimalarials. Currently, the mechanism of action for quinolon-4(1*H*)-imines **5o** and **5p** is unknown, but in contrast to their quinolone counterparts (e.g., decoquinate, **13**), it is unlikely that they target the parasite mtETC,[16,42,45] as described in the previous section.

**Metabolic and Chemical Stabilities.** The microsomal stability of a selected set of quinolon-4(1*H*)-imines was determined using rat liver microsomes. Inspection of Table 4 reveals that *N*-alkylaminequinolon-4(1*H*)-imines **5** display excellent metabolic stability, with most of the compounds

**Table 4. Results from the in Vitro Metabolism Studies Using Rat Liver Microsomes[a]**

| compd | % remaining | compd | % remaining |
|---|---|---|---|
| **5a** | 68.0 | **5l** | 65.0 |
| **5i** | 73.0 | **5r** | 62.7 |
| **5j** | 80.4 | **5t** | 81.5 |
| **5k** | 79.0 | **5u** | 75.0 |

[a]Data present the percentage of remaining compound after 6 h of incubation with microsomes in the presence of the NADPH-regenerating system.

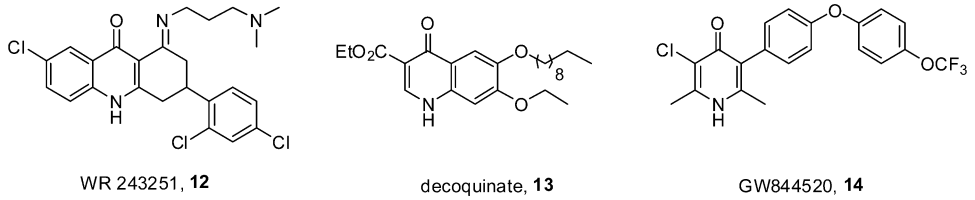


**Figure 7.** Chemical structures of *Plasmodium falciparum* $bc_1$ complex inhibitors containing dihydroacridinedione (**12**), 4(1*H*)-quinolone (**13**), and 4(1*H*)-pyridone (**14**) cores.


dx.doi.org/10.1021/jm4011466 | *J. Med. Chem.* 2013, 56, 7679−7690

presenting negligible degradation after 6 h of incubation, in contrast with the previously reported *N*-alkyl counterparts (e.g., **3**, Figure 1), which were degraded in rat liver microsomes with half-lives of ∼4 h.[24] These results also suggest that the rate of degradation is not significantly affected by the length of the aminoalkyl chain (e.g., **5j** vs **5t**) or by the nature of substituents at the quinolon-4(1*H*)-imine moiety (e.g., **5r** vs **5t**). A similar result was observed when acyclic terminal amines were replaced by cyclic amines (e.g., **5j** vs **5k**). None of the selected compounds showed any degradation in the control experiments (with the NADPH-regenerating system absent), suggesting that there was no major noncofactor dependent metabolism contributing to their degradation in liver microsomes. Furthermore, compound **5u** showed no significant degradation when incubated in pH 7.4 and 0.3 aqueous buffers at 37 °C for 10 days, suggesting that the *N*-alkylamine-quinolon-4(1*H*)-imines are stable compounds, in contrast to their *N*-Mannich-base counterparts.[18]

The MS scan data from the incubation mixtures of compound **5u** in microsomes were screened for the presence of fragments corresponding to the putative metabolites (see Supporting Information). The reaction profile of **5u** revealed the formation of the corresponding quinoline as the major metabolite, suggesting that N-dealkylation is the predominant pathway.

## CONCLUSION

We report that quinolon-4(1*H*)-imines **5** bearing an alkylamine side-chain at N-1 are a new family of efficient dual-stage antiplasmodial agents endowed with chemical and metabolic stability. Compounds **5** inhibited the development of intra-erythrocytic forms of *P. falciparum* with $IC_{50}$ values in the nanomolar range and were associated with low cytotoxicity against HEK293T mammalian cells. The length of the side chain between N-1 and the distal amine seems to be critical for activity, with side chains with three and four carbon atoms being most active. Lipophilic substituents in the iminoaryl moiety improve potency, while strong electron-withdrawing substituents at C-6 and C-7 of the quinolonimine moiety were detrimental to activity against the erythrocytic stage parasites. In spite of structural resemblance of compounds **5** to antimalarial 4-aminoquinolines, which includes the presence of two basic groups that can lead to concentration in the acidic DV of the parasite, the primary mechanism of action of quinolon-4(1*H*)-imines **5** does not appear to involve inhibition of heme crystallization. In addition, a phenotypic assay based on a *P. falciparum* cell line transfected with cytoplasmic yeast DHODH suggested that inhibition of the $bc_1$ complex is not the primary antimalarial mode of action for quinolon-4(1*H*)-imines **5**. Additional studies on the mechanism of action of new quinolon-4(1*H*)-imines are underway.

Quinolon-4(1*H*)-imines **5** were also active against the liver stage of infection. Derivative **5p** was the most promising compound, with $IC_{50}$ values of 54 and 710 nM against the erythrocytic and liver stages of infection, respectively, with minimal toxicity against human cells. Importantly, compounds **5** displayed considerable stability toward hepatic enzymes and aqueous buffers, supporting the conclusion that extending the linker between N-1 and the nitrogen atom is an effective approach to remove the source of reactivity of their *N*-Mannich-base and *N*-alkyl counterparts, **2** and **3**, respectively. Overall, our study reveals that quinolon-4(1*H*)-imines such as **5p** are a good starting point to exploit for lead optimization toward developing dual-stage antimalarials.

## EXPERIMENTAL SECTION

**Chemistry.** All manipulations requiring anhydrous conditions were carried out in flame-dried glassware, with magnetic stirring and under a nitrogen atmosphere. Chemicals and anhydrous solvents were obtained from commercial sources (Sigma-Aldrich or Alfa Aesar) and were used as received. 4,6-Dichloroquinoline (**6c**) and 4-chloro-6-(trifluoromethyl)quinolone (**6d**) were prepared according to literature procedures, and their analytical data were in agreement with those already published[26,27] (see Supporting Information). Analytical TLC plates, aluminum sheets with silica gel F250 (Merck), were visualized by UV light (254 or 366 nm) or stained with $KMnO_4$ or with a solution of ninhydrin in ethanol. Flash chromatography was performed on Kieselgel 60 $GF_{254}$ silica (Merck) of 0.040−0.063 mm.

Melting points were determined on a Kofler melting point apparatus. NMR spectra were recorded on a Bruker 400 Ultra-Shield ($^1$H, 400.13 MHz; $^{13}$C, 100.61 MHz). Data are reported as follows: chemical shift, multiplicity (s, singlet; d, doublet; t, triplet; dd, doublet of doublets; dt, doublet of triplets; q, quartet; m, multiplet; br, broad), coupling constants (*J* in Hz), integration, and assignment. Chemical shifts are given in parts per million (ppm) with the solvent signal as internal standard [$CDCl_3$ $\delta$ ($^1$H) 7.26 ppm and $\delta$ ($^{13}$C) 77.2 ppm, and $CD_3OD$ $\delta$ ($^1$H) 4.87 ppm and $\delta$ ($^{13}$C) 49.0 ppm]. High resolution mass spectrometry (HRMS) was performed on a Bruker MicrOTOF equipped with ESI ion source from the Mass Spectrometry and Proteomics Unity of the University of Santiago de Compostela, Spain. To determine the purity of the final compounds (**5a**−**v**), HPLC experiments were conducted using an ELITE LaChrom VWR HITACHI equipment (pump + controller L-2130, UV detector L-2400) and a column LiChroCART, RP-18e, 5 $\mu$m. All quinolon-4(1*H*)-imines tested in biological assays were ≥95% pure. Conditions and retention times are described in the Supporting Information.

**General Procedure A for N-Alkylated Derivatives (5a−l, 5u, 5v).** To a solution of the corresponding quinolin-4-amines in anhydrous DMF (3.0 mL/mmol), under $N_2$ atmosphere, was slowly added NaH (4.0 equiv, 40% dispersion in oil) at room temperature. The mixture was stirred until evolution of hydrogen ceased (10−60 min). The desired alkylamine chloride reagent (1.5 equiv) and NaI (3.0 equiv) were added, and the mixture was stirred at 80 °C for 5−12 h. The mixture was then concentrated under reduced pressure, diluted with DCM, and washed with brine. The aqueous phase was extracted with DCM (3 × 50 mL), and the combined organic phases were dried over $Na_2SO_4$. The crude product was then purified by flash chromatography (DCM/MeOH/TEA, 9:0.9:0.1) and recrystallized from different systems (e.g., DCM/MeOH) to afford the final pure product.

**General Procedure B for N-Alkylated Derivatives (5q−t).** To a solution of the corresponding quinolin-4-amines in anhydrous DMF (3 mL/mmol), under $N_2$ atmosphere, was slowly added NaH (4 equiv, 40% dispersion in oil) at room temperature. The mixture was stirred until evolution of hydrogen ceased (10−60 min). The desired alkyl dibromide reagent (1.5 equiv) was then added, and the mixture was stirred at room temperature. The mixture was then concentrated under reduced pressure, diluted with DCM, and washed with brine. The aqueous phase was extracted with DCM (3 × 50 mL), and the combined organic phases were dried over $Na_2SO_4$. The resulting product and NaI (1.5 equiv) were then dissolved in DEA (15 mL/mmol) and stirred at room temperature for 78 h. The mixture was concentrated under reduced pressure and the crude product was purified by flash chromatography (DCM/MeOH/$Et_3N$, 9:0.9:0.1) and recrystallized from different systems (e.g., DCM/MeOH) to afford the final pure product.

**General Procedure for Suzuki Coupling (5m−p).** To a solution of the aryl halide in dry 1,4-dioxane at room temperature was consecutively added $PdCl_2(Ph_3P)_2$ (0.1 equiv), *t*-Bu-Xphos (0.1 equiv), $Na_2CO_3$ 1 M (3 equiv), and boronic acid (1.2 equiv). After degassing for 5 min, the resulting mixture was heated at 100 °C under


dx.doi.org/10.1021/jm4011466 | J. Med. Chem. 2013, 56, 7679−7690

$N_2$ atmosphere overnight. The mixture was then cooled to room temperature, diluted with DCM, and filtered through a pad of Celite. The filtrate was concentrated under reduce pressure and the crude product was purified by thin layer chromatography (DCM/MeOH/$Et_3N$, 95:4:1) to afford the corresponding 7-substituted quinolin-4-imines.

**(*E*)-*N*-(7-Chloro-1-(2-(diethylamino)ethyl)quinolin-4(1*H*)-ylidene)biphenyl-4-amine (5a).** According to general procedure A, the product was obtained as a yellow solid (37 mg, 11%). Mp 115−117 °C. $^1$H NMR ($CD_3OD$) $\delta$ 8.68 (d, $J$ = 8.8 Hz, 1H), 8.43 (d, $J$ = 7.6 Hz, 1H), 8.37 (s, 1H), 7.90−7.86 (m, 3H), 7.72−7.70 (m, 2H), 7.58−7.56 (m, 2H), 7.52−7.49 (m, 2H), 7.43−7.41 (m, 1H), 6.98 (d, $J$ = 7.2 Hz, 1H), 4.66 (t, $J$ = 5.6 Hz, 2H), 2.90 (t, $J$ = 5.6 Hz, 2H), 2.58−2.53 (m, 4H), 0.87−0.83 (m, 6H). $^{13}$C NMR ($CD_3OD$) $\delta$ 154.3, 148.4, 140.8, 139.3, 135.9, 128.7, 128.3, 127.7, 127.6, 126.6, 125.7, 125.5, 117.9, 99.9, 53.3, 51.2, 46.9, 10.9. HRMS (ESI) $m/z$ calcd for $[C_{27}H_{29}ClN_3]^+$, 430.2045 [M + H$^+$]; found, 430.2032.

**(*E*)-*N*-(7-Chloro-1-(2-(pyrrolidin-1-yl)ethyl)quinolin-4(1*H*)-ylidene)biphenyl-4-amine (5b).** According to general procedure A, the product was obtained as a yellow solid (49 mg, 39%). Mp 221−224 °C. $^1$H NMR ($CD_3OD$) $\delta$ 8.56 (d, $J$ = 9.0 Hz, 1H), 7.71−7.55 (m, 4H), 7.45 (t, $J$ = 7.7 Hz, 2H), 7.38−7.21 (m, 3H), 7.02 (d, $J$ = 8.4 Hz, 2H), 6.92 (d, $J$ = 8.0 Hz, 1H), 6.02 (d, $J$ = 8.0 Hz, 1H), 3.99 (t, $J$ = 7.1 Hz, 2H), 2.86 (t, $J$ = 7.1 Hz, 2H), 2.60 (d, $J$ = 5.3 Hz, 4H), 1.91−1.73 (m, 4H). $^{13}$C NMR ($CD_3OD$) $\delta$ 154.6, 152.4, 141.6, 140.2, 140.0, 137.4, 135.3, 129.0, 128.4, 128.2, 127.0, 126.9, 124.3, 124.0, 122.1, 114.4, 101.7, 54.9, 54.3, 51.8, 23.9. HRMS (ESI) $m/z$ calcd for $[C2_7H_{27}ClN_3]^+$, 428.1888 [M + H$^+$]; found, 428.1898.

**(*E*)-*N*-(7-Chloro-1-(3-(piperidin-1-yl)propyl)quinolin-4(1*H*)-ylidene)biphenyl-4-amine (5c).** According to general procedure A, the product was obtained as a yellow solid (50 mg, 48%). Mp 176−178 °C. $^1$H NMR ($CDCl_3$) $\delta$ 8.56 (d, $J$ = 8.7 Hz, 1H), 7.67−7.57 (m, 4H), 7.46 (t, $J$ = 7.7 Hz, 2H), 7.35−7.20 (m, 3H), 7.06−6.95 (m, 3H), 6.00 (d, $J$ = 8.0 Hz, 1H), 3.98 (t, $J$ = 6.6 Hz, 2H), 2.37 (br, 4H), 2.31 (t, $J$ = 6.5 Hz, 2H), 1.97−1.91 (m, 2H), 1.65−1.56 (m, 4H), 1.47 (br, 2H). $^{13}$C NMR ($CDCl_3$) $\delta$ 154.4, 152.2, 141.3, 140.0, 137.1, 134.9, 128.7, 128.0, 127.9, 126.9, 127.0, 127.0, 124.1, 123.6, 121.8, 114.4, 101.0, 54.9, 54.5, 49.6, 26.1, 25.6, 24.5. HRMS (ESI) $m/z$ calcd for $[C_{29}H_{31}ClN_3]^+$, 456.2201 [M + H$^+$]; found, 456.2199.

**(*E*)-4-Chloro-*N*-(7-chloro-1-(3-(piperidin-1-yl)propyl)-quinolin-4(1*H*)-ylidene)aniline (5d).** According to general procedure A, the product was obtained as a yellow solid (205 mg, 34%). Mp 157−159 °C. $^1$H NMR ($CDCl_3$) $\delta$ 8.55 (d, $J$ = 8.7 Hz, 1H), 7.36 (s, 1H), 7.33−7.20 (m, 3H), 7.06 (d, $J$ = 8.0 Hz, 1H), 6.96−6.83 (m, 2H), 5.90 (d, $J$ = 8.0 Hz, 1H), 4.00 (t, $J$ = 6.6 Hz, 2H), 2.36 (br, 4H), 2.30 (t, $J$ = 6.5 Hz, 2H), 1.93 (dt, $J$ = 13.1, 6.5 Hz, 2H), 1.62 (dt, $J$ = 10.9, 5.5 Hz, 4H), 1.47 (br, 2H). $^{13}$C NMR ($CDCl_3$) $\delta$ 154.8, 148.9, 140.4, 139.8, 137.4, 129.3, 128.0, 127.3, 123.9, 123.4, 123.0, 114.5, 100.6, 54.8, 54.5, 49.7, 26.1, 25.5, 24.5. HRMS (ESI) $m/z$ calcd for $[C_{23}H_{26}Cl_2N_3]^+$, 414.1498 [M + H$^+$]; found, 414.1497.

**(*E*)-4-Bromo-*N*-(7-chloro-1-(3-(piperidin-1-yl)propyl)-quinolin-4(1*H*)-ylidene)aniline (5e).** According to general procedure A, the product was obtained as a yellow solid (133 mg, 29%). Mp 165−167 °C. $^1$H NMR ($CDCl_3$) $\delta$ 8.55 (d, $J$ = 8.7 Hz, 1H), 7.49−7.40 (m, 2H), 7.36 (d, $J$ = 1.8 Hz, 1H), 7.31−7.21 (m, 1H), 7.06 (d, $J$ = 8.0 Hz, 1H), 6.85 (t, $J$ = 5.7 Hz, 2H), 5.90 (d, $J$ = 8.0 Hz, 1H), 4.00 (t, $J$ = 6.5 Hz, 2H), 2.36 (br, 4H), 2.29 (t, $J$ = 6.5 Hz, 2H), 1.96−1.91 (m, 2H), 1.69−1.56 (m, 4H), 1.47 (br, 2H). $^{13}$C NMR ($CDCl_3$) $\delta$ 154.7, 140.5, 139.8, 137.4, 132.3, 128.0, 123.9, 123.5, 114.9, 114.6, 100.6, 54.8, 54.5, 49.7, 26.1, 25.5, 24.5. HRMS (ESI) $m/z$ calcd for $[C_{23}H_{26}BrClN_3]^+$, 460.0973 [M + H$^+$]; found, 460.0965.

**(*E*)-*N*-(7-Chloro-1-(3-(piperidin-1-yl)propyl)quinolin-4(1*H*)-ylidene)aniline (5f).** According to general procedure A, the product was obtained as a yellow solid (133 mg, 40%). Mp 137−139 °C. $^1$H NMR ($CDCl_3$) $\delta$ 8.55 (d, $J$ = 8.7 Hz, 1H), 7.41−7.32 (m, 3H), 7.24 (dd, $J$ = 8.7, 1.9 Hz, 1H), 7.09−7.03 (m, 1H), 7.02−6.87 (m, 3H), 5.91 (d, $J$ = 8.0 Hz, 1H), 3.97 (t, $J$ = 6.5 Hz, 2H), 2.39 (br, 4H), 2.29 (t, $J$ = 6.5 Hz, 2H), 2.00−1.83 (m, 2H), 1.69−1.54 (m, 4H), 1.46 (br, 2H). $^{13}$C NMR ($CDCl_3$) $\delta$ 154.4, 140.0, 137.0, 129.3, 127.9, 123.8, 123.6, 122.2, 121.5, 114.4, 100.9, 54.8, 54.5, 49.5, 26.1, 25.5, 24.5. HRMS (ESI) $m/z$ calcd for $[C_{23}H_{27}ClN_3]^+$, 380.1888 [M + H$^+$]; found, 380.1881.

**(*E*)-*N*-(7-Chloro-1-(3-(piperidin-1-yl)propyl)quinolin-4(1*H*)-ylidene)-4-methylaniline (5g).** According to general procedure A, the product was obtained as a yellow solid (30 mg, 20%). Mp 164−166 °C. $^1$H NMR ($CDCl_3$) $\delta$ 8.59 (d, $J$ = 8.4 Hz, 1H), 7.33 (d, $J$ = 1.7 Hz, 1H), 7.24 (dd, $J$ = 8.4, 1.7 Hz, 1H), 7.16 (d, $J$ = 7.9 Hz, 2H), 6.99 (d, $J$ = 7.9 Hz, 1H), 6.87 (d, $J$ = 8.0 Hz, 2H), 5.96 (d, $J$ = 8.0 Hz, 1H), 3.98 (t, $J$ = 6.6 Hz, 2H), 2.36 (br, 4H), 2.36 (br, 3H), 2.29 (t, $J$ = 6.5 Hz, 2H), 1.95−1.89 (m, 2H), 1.67−1.54 (m, 4H), 1.46 (br, 2H). $^{13}$C NMR ($CDCl_3$) $\delta$ 154.4, 140.0, 139.9, 137.1, 131.7, 130.0, 128.0, 123.7, 121.4, 114.4, 100.9, 54.8, 54.5, 49.6, 26.1, 25.5, 24.4, 20.9. HRMS (ESI) $m/z$ calcd for $[C_{24}H_{29}ClN_3]^+$, 394.2045 [M + H$^+$]; found, 394.2040.

**(*E*)-*N*-(7-Chloro-1-(3-(piperidin-1-yl)propyl)quinolin-4(1*H*)-ylidene)-4-fluoroaniline (5h).** According to general procedure A, the product was obtained as a yellow solid (38 mg, 15%). Mp 123−125 °C. $^1$H NMR ($CDCl_3$) $\delta$ 8.55 (d, $J$ = 8.6 Hz, 1H), 7.34 (s, 1H), 7.32−7.18 (m, 1H), 7.06−7.02 (m, 3H), 6.89 (dd, $J$ = 7.6, 5.2 Hz, 2H), 5.90 (d, $J$ = 7.9 Hz, 1H), 3.99 (t, $J$ = 6.4 Hz, 2H), 2.36 (br, 4H), 2.30 (t, $J$ = 6.4 Hz, 2H), 2.04−1.85 (m, 2H), 1.64−1.59 (m, 4H), 1.47 (br, 2H). $^{13}$C NMR ($CDCl_3$) $\delta$ 160.0, 157.6, 154.9, 140.2, 139.9, 137.2, 127.9, 123.8, 123.4, 122.6, 115.7, 114.5, 100.6, 54.8, 54.5, 49.6, 26.1, 25.5, 24.5. HRMS (ESI) $m/z$ calcd for $[C_{23}H_{26}ClFN_3]^+$, 398.1794[M + H$^+$]; found, 398.1788.

**(*E*)-*N*-(7-Chloro-1-(3-(piperidin-1-yl)propyl)quinolin-4(1*H*)-ylidene)-4-phenoxyaniline (5i).** According to general procedure A, the product was obtained as a yellow solid (42 mg, 21%). Mp 154−156 °C. $^1$H NMR ($CDCl_3$) $\delta$ 8.84 (d, $J$ = 8.7 Hz, 1H), 7.49 (s, 1H), 7.45−7.31 (m, 4H), 7.17−6.95 (m, 7H), 6.19 (d, $J$ = 7.7 Hz, 1H), 4.15 (t, $J$ = 6.2 Hz, 2H), 2.36 (br, 4H), 2.30 (t, $J$ = 6.2 Hz, 2H), 2.05−1.89 (m, 2H), 1.69−1.55 (m, 4H), 1.47 (br, 2H). $^{13}$C NMR ($CDCl_3$) $\delta$ 157.8, 154.8, 153.2, 141.8, 139.7, 138.3, 129.7, 128.4, 124.9, 123.9, 122.9, 122.0, 120.2, 118.3, 115.0, 100.7, 54.7, 54.5, 50.4, 26.1, 25.6, 24.4. HRMS (ESI) $m/z$ calcd for $[C_{29}H_{31}ClN_3O]^+$, 472.2150 [M + H$^+$]; found, 472.2159.

**(*E*)-*N*-(1-(2-(Diethylamino)ethyl)-7-(trifluoromethyl)quinolin-4(1*H*)-ylidene)biphenyl-4-amine (5j).** According to general procedure A, the product was obtained as a yellow solid (97 mg, 21%). Mp 148−150 °C. $^1$H NMR ($CD_3OD$) $\delta$ 8.94 (d, $J$ = 8.8 Hz, 1H), 8.71 (d, $J$ = 7.6 Hz, 1H), 8.55 (s, 1H), 8.15 (d, $J$ = 8.8 Hz, 1H), 7.89−7.87 (m, 2H), 7.72−7.70 (m, 2H), 7.66−7.62 (m, 2H), 7.52−7.48 (m, 2H),7.42−7.40 (m, 1H), 7.11 (d, $J$ = 7.6 Hz, 1H), 5.29 (br, 2H), 3.54 (br, 2H), 3.19 (br, 2H), 1.26 (br, 6H). $^{13}$C NMR ($CD_3OD$) $\delta$ 155.7, 148.8, 141.3, 139.6, 135.5, 128.7, 128.4, 127.6, 126.6, 126.2, 125.6, 123.0, 120.9, 115.6, 101.7, 49.9, 48.1, 47.0, 18.8. HRMS (ESI) $m/z$ calcd for $[C_{28}H_{29}F_3N_3]^+$, 464.2308 [M + H$^+$]; found, 464.2315.

**(*E*)-*N*-(1-(2-(Pyrrolidin-1-yl)ethyl)-7-(trifluoromethyl)-quinolin-4(1*H*)-ylidene)biphenyl-4-amine (5k).** According to general procedure A, the product was obtained as a yellow solid (37 mg, 30%). Mp 238−240 °C. $^1$H NMR ($CD_3OD$) $\delta$ 8.92 (d, $J$ = 8.8 Hz, 1H), 8.72 (d, $J$ = 7.2 Hz, 1H), 8.55 (s, 1H), 8.13 (d, $J$ = 8.8 Hz, 1H), 7.87 (d, $J$ = 8.4 Hz, 2H), 7.70 (d, $J$ = 7.6 Hz, 2H), 7.63 (d, $J$ = 8.4 Hz, 2H), 7.49 (t, $J$ = 7.6 Hz, 2H), 7.40 (t, $J$ = 7.6 Hz, 1H), 7.09 (d, $J$ = 7.2 Hz, 1H), 4.99 (t, $J$ = 6.4 Hz, 2H), 3.39 (br, 2H), 3.01 (br, 4H), 1.95 (m, 4H). $^{13}$C NMR ($CD_3OD$) $\delta$ 155.6, 148.6, 141.5, 139.6, 138.3, 135.7, 135.3, 128.7, 128.3, 127.6, 126.6, 126.1, 125.6, 124.6, 122.9, 115.8, 101.6, 54.0, 53.2, 52.0, 23.0. HRMS (ESI) $m/z$ calcd for $[C_{28}H_{27}F_3N_3]^+$, 462.2152 [M + H$^+$]; found, 462.2146.

**(*E*)-*N*-(1-(3-(Piperidin-1-yl)propyl)-7-(trifluoromethyl)-quinolin-4(1*H*)-ylidene)biphenyl-4-amine (5l).** According to general procedure A, the product was obtained as a yellow solid (33 mg, 21%). Mp 174−177 °C. $^1$H NMR ($CDCl_3$) $\delta$ 8.74 (d, $J$ = 8.3 Hz, 1H), 7.68−7.58 (m, 4H), 7.56−7.49 (m, 2H), 7.49−7.41 (m, 2H), 7.36−7.30 (m, 1H), 7.12−6.99 (m, 3H), 6.05 (d, $J$ = 8.0 Hz, 1H), 4.06 (t, $J$ = 6.5 Hz, 2H), 2.36 (br, 2H), 2.32 (t, $J$ = 6.5 Hz, 2H), 1.98−1.92 (m, 2H), 1.64−1.55 (m, 4H), 1.47 (br, 2H). $^{13}$C NMR ($CDCl_3$) $\delta$ 154.2, 152.0, 141.2, 140.4, 138.2, 135.1, 132.7, 132.4, 128.7, 128.0, 127.6, 126.7, 126.6, 125.3, 123.0, 122.6, 121.6, 119.3, 111.8, 111.8,


dx.doi.org/10.1021/jm4011466 | J. Med. Chem. 2013, 56, 7679−7690

101.2, 54.9, 54.5, 49.6, 26.1, 25.4, 24.5. HRMS (ESI) $m/z$ calcd for $[C_{30}H_{31}F_3N_3]^+$, 490.2465 [M + H$^+$]; found, 490.2465.

**(*E*)-*N*-(7-(4-Fluorophenyl)-1-(3-(piperidin-1-yl)propyl)-quinolin-4(1*H*)-ylidene)aniline (5m).** Yellow solid (32 mg, 80%). Mp 132−134 °C. $^1$H NMR ($CD_3OD$) $\delta$ 8.68 (d, $J$ = 8.6 Hz, 1H), 8.49 (d, $J$ = 7.2 Hz, 1H), 8.28 (s, 1H), 8.10 (d, $J$ = 8.6 Hz, 1H), 7.97−7.89 (m, 2H), 7.62−7.54 (m, 2H), 7.50−7.42 (m, 3H), 7.31 (t, $J$ = 8.4 Hz, 2H), 6.84 (d, $J$ = 7.2 Hz, 1H), 4.74 (t, $J$ = 6.8 Hz, 2H), 2.65−2.30 (m, 6H), 2.24−2.15 (m, 2H), 1.57−1.48 (m, 4H), 1.43 (br, 2H). $^{13}$C NMR ($CD_3OD$) $\delta$ 165.1, 156.9, 148.6, 147.7, 140.4, 138.4, 136.1, 131.4, 131.1, 129.3, 127.7, 126.7, 125.9, 118.9, 117.3, 116.7, 101.4, 56.1, 55.4, 54.0, 26.7, 26.3, 24.8. HRMS (ESI) $m/z$ calcd for $[C_{29}H_{31}FN_3]^+$, 440.2497 [M + H]$^+$; found, 440.2498.

**(*E*)-*N*-(7-(4-Fluorophenyl)-1-(3-(piperidin-1-yl)propyl)-quinolin-4(1*H*)-ylidene)-[1,1′-biphenyl]-4-amine (5n).** Yellow solid (52 mg, 76%). Mp 158−160 °C. $^1$H NMR ($CD_3OD$) $\delta$ 8.73 (d, $J$ = 8.8 Hz, 1H), 8.54 (d, $J$ = 7.4 Hz, 1H), 8.33 (s, 1H), 8.15 (d, $J$ = 8.8 Hz, 1H), 8.00−7.93 (m, 2H), 7.87 (d, $J$ = 8.5 Hz, 2H), 7.71 (d, $J$ = 7.6 Hz, 2H), 7.58 (d, $J$ = 8.5 Hz, 2H), 7.50 (t, $J$ = 7.6 Hz, 2H), 7.44−7.32 (m, 3H), 6.98 (d, $J$ = 7.4 Hz, 1H), 4.78 (t, $J$ = 7.0 Hz, 2H), 2.52−2.32 (m, 6H), 2.26−2.16 (m, 2H), 1.58−1.50 (m, 4H), 1.46 (br, 2H). $^{13}$C NMR ($CD_3OD$) $\delta$ 165.4, 157.1, 148.8, 148.0, 142.6, 141.4, 140.7, 137.8, 136.4, 131.4, 130.4, 130.0, 129.2, 128.2, 128.0, 127.2, 126.2, 119.2, 117.5, 116.9, 101.8, 56.1, 55.4, 54.1, 26.7, 26.2, 24.7. HRMS (ESI) $m/z$ calcd for $[C_{35}H_{35}FN_3]^+$, 516.2810 [M + H]$^+$; found, 516.2800.

**(*E*)-4-([1,1′-Biphenyl]-4-ylimino)-1-(3-(piperidin-1-yl)propyl)-*N*-(pyridin-2-yl)-1,4-dihydroquinolin-7-amine (5o).** Yellow solid (16 mg, 24%). Mp 172−174 °C. $^1$H NMR ($CD_3OD$) $\delta$ 9.21 (s, 1H), 8.46 (d, $J$ = 9.3 Hz, 1H), 8.40 (d, $J$ = 4.3 Hz, 1H), 8.36 (d, $J$ = 7.4 Hz, 1H), 7.82 (d, $J$ = 8.4 Hz, 2H), 7.77−7.66 (m, 4H), 7.53 (d, $J$ = 8.4 Hz, 2H), 7.48 (t, $J$ = 7.6 Hz, 2H), 7.39 (t, $J$ = 7.6 Hz, 1H), 7.11−6.95 (m, 2H), 6.81 (d, $J$ = 7.4 Hz, 1H), 4.58 (t, $J$ = 7.0 Hz, 2H), 2.73−2.58 (m, 2H), 2.55 (br, 4H), 2.39−2.23 (m, 2H), 1.66−1.54 (m, 4H), 1.48 (br, 2H). $^{13}$C NMR ($CD_3OD$) $\delta$ 156.4, 155.7, 148.9, 148.5, 147.3, 141.9, 141.9, 141.2, 139.2, 137.8, 130.1, 129.6, 128.9, 128.0, 126.9, 125.6, 120.6, 118.1, 113.9, 113.2, 102.7, 100.3, 56.5, 55.3, 54.3, 26.2, 25.8, 24.8. HRMS (ESI) $m/z$ calcd for $[C_{34}H_{36}N_5]^+$, 514.2965 [M + H]$^+$; found, 514.2966.

**(*E*)-*N*-(1′-(3-(Piperidin-1-yl)propyl)-[3,7′-biquinolin]-4′(1′*H*)-ylidene)-[1,1′-biphenyl]-4-amine (5p).** Orange solid (69 mg, 62%). Mp 152−154 °C. $^1$H NMR ($CDCl_3$) 9.23 (d, $J$ = 2.1 Hz, 1H), 8.86 (d, $J$ = 7.1 Hz, 1H), 8.40 (d, $J$ = 2.1 Hz, 1H), 8.18 (d, $J$ = 8.4 Hz, 1H), 7.94 (d, $J$ = 7.9 Hz, 1H), 7.77 (t, $J$ = 8.4 Hz, 1H), 7.70−7.58 (m, 7H), 7.43 (t, $J$ = 7.6 Hz, 2H), 7.31 (t, $J$ = 7.6 Hz, 1H), 7.18 (d, $J$ = 7.5 Hz, 1H), 7.11 (d, $J$ = 8.0 Hz, 2H), 6.12 (d, $J$ = 7.5 Hz, 1H), 4.16 (t, $J$ = 6.3 Hz, 2H), 2.42−2.26 (m, 6H), 2.05−1.97 (m, 2H), 1.55−1.47 (m, 4H), 1.44−1.34 (br, 2H). $^{13}$C NMR ($CDCl_3$) $\delta$ 155.0, 149.7, 147.8, 141.2, 140.9, 140.9, 139.6, 135.4, 135.2, 134.0, 133.2, 130.0, 129.4, 128.8, 128.2, 128.0, 128.0, 127.7, 127.4, 126.8, 126.7, 124.6, 123.0, 122.4, 113.5, 100.8, 55.0, 54.9, 50.1, 26.1, 25.7, 24.5. HRMS (ESI) $m/z$ calcd for $[C_{38}H_{37}N_4]^+$, 549.3013 [M + H]$^+$; found, 549.3003.

**(*E*)-*N*-(7-Chloro-1-(3-(diethylamino)propyl)quinolin-4(1*H*)-ylidene)biphenyl-4-amine (5q).** According to general procedure B, the product was obtained as a yellow solid (16 mg, 8%). Mp 95−98 °C. $^1$H NMR ($CDCl_3$) $\delta$ 8.68 (d, $J$ = 8.9 Hz, 1H), 7.73−7.52 (m, 4H), 7.52−7.41 (m, 3H), 7.41−7.22 (m, 2H), 7.17−7.05 (m, 3H), 6.09 (d, $J$ = 7.7 Hz, 1H), 4.02 (t, $J$ = 6.6 Hz, 2H), 2.56 (dd, $J$ = 14.1, 7.0 Hz, 4H), 2.47 (t, $J$ = 6.2 Hz, 2H), 1.98−1.84 (m, 2H), 1.10−0.94 (m, 6H). $^{13}$C NMR ($CDCl_3$) $\delta$ 154.6, 141.4, 140.6, 139.7, 137.6, 128.7, 128.2, 128.0, 126.7, 124.0, 122.2, 119.9, 114.6, 101.0, 50.3, 49.3, 46.4, 26.2, 11.5. HRMS (ESI) $m/z$ calcd for $[C_{28}H_{31}ClN_3]^+$, 444.2201 [M + H$^+$]; found, 444.2200.

**(*E*)-*N*-(7-Chloro-1-(4-(diethylamino)butyl)quinolin-4(1*H*)-ylidene)biphenyl-4-amine (5r).** According to general procedure B, the product was obtained as a yellow solid (34 mg, 12%). Mp 108−110 °C. $^1$H NMR ($CDCl_3$) $\delta$ 8.59 (d, $J$ = 8.7 Hz, 1H), 7.72−7.57 (m, 4H), 7.52−740 (m, 2H), 7.37−7.33 (m, 2H), 7.29−7.24 (m, 2H), 7.04 (d, $J$ = 8.3 Hz, 2H), 6.93 (d, $J$ = 8.0 Hz, 1H), 6.03 (d, $J$ = 8.0 Hz, 1H), 3.99−3.83 (m, 2H), 2.55 (q, $J$ = 7.1 Hz, 4H), 2.48 (t, $J$ = 7.1 Hz, 2H), 1.84 (dt, $J$ = 15.0, 7.6 Hz, 2H), 1.63−1.52 (m, 2H), 1.12−0.97 (m, 6H). $^{13}$C NMR ($CDCl_3$) $\delta$ 154.4, 151.6, 141.2, 139.7, 137.2, 135.1, 132.7, 128.7, 128.1, 127.9, 126.7, 126.6, 123.8, 121.9, 114.5, 101.2, 52.4, 52.1, 46.8, 26.4, 24.4, 11.6. HRMS (ESI) $m/z$ calcd for $[C_{29}H_{33}ClN_3]^+$, 458.2358 [M + H$^+$]; found, 458.2360.

**(*E*)-*N*-(1-(3-(Diethylamino)propyl)-7-(trifluoromethyl)-quinolin-4(1*H*)-ylidene)biphenyl-4-amine (5s).** According to general procedure B, the product was obtained as a yellow solid (34 mg, 4%). Mp 97−99 °C. $^1$H NMR ($CDCl_3$) $\delta$ 9.28 (d, $J$ = 8.8 Hz, 1H), 7.98 (s, 1H), 7.77−7.71 (m, 2H), 7.63−7.58 (m, 4H), 7.47−7.38 (m, 2H), 7.36−7.31 (m, 3H), 6.63 (d, $J$ = 7.2 Hz, 1H), 4.43 (t, $J$ = 6.8 Hz, 2H), 2.68−2.67 (m, 4H), 2.61 (t, $J$ = 6.4 Hz, 2H), 2.08 (t, $J$ = 6.4 Hz, 2H), 1.09−1.05 (m, 6H). $^{13}$C NMR ($CDCl_3$) $\delta$ 154.8, 146.4, 140.1, 139.6, 138.0, 129.0, 128.4, 127.8, 126.8, 124.9, 124.3, 122.8, 121.8, 114.2, 101.6, 52.1, 49.0, 46.7, 26.1, 10.3. HRMS (ESI) $m/z$ calcd for $[C_{29}H_{31}F_3N_3]^+$, 478.2465 [M + H$^+$]; found, 478.2470.

**(*E*)-*N*-(1-(4-(Diethylamino)butyl)-7-(trifluoromethyl)-quinolin-4(1*H*)-ylidene)biphenyl-4-amine (5t).** According to general procedure B, the product was obtained as a yellow solid (74 mg, 15%). Mp 135−137 °C. $^1$H NMR ($CDCl_3$) $\delta$ 8.74 (d, $J$ = 8.7 Hz, 1H), 7.79−7.57 (m, 4H), 7.55−7.49 (m, 2H), 7.45 (t, $J$ = 7.6 Hz, 2H), 7.33 (t, $J$ = 6.8 Hz, 1H), 7.03 (d, $J$ = 8.3 Hz, 2H), 6.96 (d, $J$ = 8.0 Hz, 1H), 6.05 (d, $J$ = 8.0 Hz, 1H), 3.97 (t, $J$ = 7.3 Hz, 2H), 2.54 (dd, $J$ = 14.2, 7.1 Hz,4H), 2.48 (t, $J$ = 7.1 Hz, 2H), 1.85 (dt, $J$ = 14.6, 7.3 Hz, 2H), 1.59 (dd, $J$ = 14.2, 7.1 Hz, 2H), 1.04 (t, $J$ = 7.1 Hz, 6H). $^{13}$C NMR ($CDCl_3$) $\delta$ 154.1, 151.9, 141.2, 139.8, 138.5, 135.2, 132.7, 128.7, 128.0, 127.6, 126.7, 126.6, 125.3, 121.6, 119.4, 111.7, 101.6, 52.4, 52.1, 46.8, 26.5, 24.5, 11.5. HRMS (ESI) $m/z$ calcd for $[C_{30}H_{33}F_3N_3]^+$, 492.2621 [M + H$^+$]; found, 492.2629.

**(*E*)-*N*-(6-Chloro-1-(3-(piperidin-1-yl)propyl)quinolin-4(1*H*)-ylidene)biphenyl-4-amine (5u).** According to general procedure A, the product was obtained as a yellow solid (128 mg, 43%). Mp 48−50 °C. $^1$H NMR ($CDCl_3$) $\delta$ 8.66 (s, 1H), 7.70−7.52 (m, 4H), 7.53−7.40 (m, 3H), 7.38−7.24 (m, 2H), 7.12−6.98 (m, 3H), 6.03 (d, $J$ = 7.8 Hz, 1H), 4.02 (t, $J$ = 6.4 Hz, 2H), 2.36 (br, 4H), 2.30 (t, $J$ = 6.4 Hz, 2H), 1.93 (dd, $J$ = 12.6, 6.4 Hz, 2H), 1.67−1.53 (m, 4H), 1.47 (br, 2H). $^{13}$C NMR ($CDCl_3$) $\delta$ 154.2, 151.5, 141.2, 140.2, 137.5, 135.1, 131.0, 129.4, 128.7, 127.9, 126.7, 126.6, 126.5, 125.8, 121.9, 116.4, 100.6, 54.8, 54.5, 49.8, 26.1, 25.6, 24.4. HRMS (ESI) $m/z$ calcd for $[C_{29}H_{31}ClN_3]^+$, 456.2201 [M + H$^+$]; found, 456.2207.

**(*E*)-*N*-(1-(3-(Piperidin-1-yl)propyl)-6-(trifluoromethyl)-quinolin-4(1*H*)-ylidene)biphenyl-4-amine (5v).** According to general procedure A, the product was obtained as a yellow solid (47 mg, 12%). Mp 85−87 °C. $^1$H NMR ($CDCl_3$) $\delta$ 8.93 (s, 1H), 7.74 (d, $J$ = 9.0 Hz, 1H), 7.70−7.56 (m, 4H), 7.52−7.39 (m, 3H), 7.39−7.26 (m, 1H), 7.04 (t, $J$ = 7.2 Hz, 3H), 6.05 (d, $J$ = 8.0 Hz, 1H), 4.04 (t, $J$ = 6.5 Hz, 2H), 2.37 (br, 4H), 2.32 (t, $J$ = 6.5 Hz, 2H), 2.02−1.88 (m, 2H), 1.66−1.54 (m, 4H), 1.47 (br, 2H). $^{13}$C NMR ($CDCl_3$) $\delta$ 154.2, 151.8, 141.2, 140.2, 135.1, 128.7, 128.0, 126.7, 126.6, 125.5, 125.3, 124.2, 121.7, 115.2, 101.6, 54.8, 54.5, 49.7, 26.1, 25.4, 24.4. HRMS (ESI) $m/z$ calcd for $[C_{30}H_{31}F_3N_3]^+$, 490.2465 [M + H$^+$]; found, 490.2473.

**In Vitro Cytotoxicity.** The cytotoxicity was assessed using general cell viability end point MTT (3-(4,5-dimethyl-2-thiazolyl)-2,5-diphenyl-2*H*-tetrazolium bromide). Briefly, the day before experiment, cells HEK293T (human embryonic kidney epithelial cell line, ATCC CRL-11268) were seeded in 96-well tissue culture plates, in RPMI 1640 culture medium supplemented with 10% fetal serum bovine, 100 units of penicillin G (sodium salt), 100 $\mu$g/mL streptomycin sulfate, and 2 mM L-glutamine, at a concentration that allowed cells to grow exponentially during the time of the assay. Compounds to be tested were diluted in DMSO and then serially diluted in the culture medium. Compounds at different concentrations and DMSO were then added to the cells, which were incubated at 37 °C in humidified 5% $CO_2$ atmosphere. After 48 h, cell medium containing DMSO (for control cells) or tested compound solution (for test cells) was removed and replaced with fresh medium containing MTT dye. After 3 h of incubation the complete medium was removed and the intracellular formazan crystals were solubilized and extracted with DMSO. After 15 min at room temperature the absorbance was measured at 570 nm in a


dx.doi.org/10.1021/jm4011466 | J. Med. Chem. 2013, 56, 7679−7690

microplate reader. The percentage of cell viability was determined for each concentration of tested compound as described previously. The concentration of a compound reflecting a 50% inhibition of cell viability (i.e., $EC_{50}$) was determined from the concentration−response curve, applying a nonlinear regression procedure to the concentration response data using GraphPad Prism software.

**In Vitro Blood Stage Activity Assays.** Human red blood cells infected with 1% ring-stage *P. falciparum* strains synchronized with 5% sorbitol were incubated with tested compounds in 96-well plates at 37 °C for 48 h in RPMI-1640 medium, supplemented with 25 mM HEPES, pH 7.4, 10% heat inactivated human serum (or 0.5% AlbuMAX, 2% human serum), and 100 μM hypoxanthine under an atmosphere of 3% $O_2$, 5% $CO_2$, 91% $N_2$. After 48 h, the cells were fixed in 2% formaldehyde in PBS, transferred into PBS with 100 mM $NH_4Cl$, 0.1% Triton X-100, 1 nM YOYO-1, and then analyzed in a flow cytometer (FACSort, Beckton Dickinson; excitation 488 nm, emission 520 nm). Values of $IC_{50}$ were calculated using GraphPad Prism software.

**Hemozoin-like Crystals Growth Inhibition.** Inhibition of hemozoin-like crystals formation by tested compounds was assessed using the previously described in vitro method.[36] In short, a hemozoin-like crystals stock suspension was sonicated for 3 min and diluted in fresh broth medium to a final concentration of 2 μM (heme equivalents) in the wells of a 96-well plate. Stock solutions of tested compounds were prepared at 25 mM in DMSO. Stock solutions of chloroquine (positive control) and gentamicin (negative control) were prepared at 100 mM in distilled water, and all were 0.22-μm-filtered previous to being diluted to 0−1000 μM final concentration in the wells. Plates were incubated at 37 °C in a 5% $CO_2$ atmosphere for 5 days to observe the presence or absence of crystal growth. All tests were performed in triplicate.

**Growth Inhibition against Transgenic *P. falciparum*.** 3D7-yDHOD·GFP, a transgenic derivative of *P. falciparum* 3D7 containing yeast dihydroorotate dehydrogenase (DHODH), was generated via the electroporation of purified pHHyDHOD-GFP plasmid into ring stages of *P. falciparum* using a Bio-Rad GenePulser as described previously.[46] *P. falciparum* cell extracts and measurement of cytochrome *c* reductase activity was performed as described previously.[41,48]

**In Vitro Liver Stage Activity Assays.** Huh-7 cells, a human hepatoma cell line, were cultured in 1640 RPMI medium supplemented with 10% v/v fetal calf serum (FCS), 1% v/v nonessential amino acids, 1% v/v penicillin/streptomycin, 1% v/v glutamine, and 10 mM 4-(2-hydroxyethyl)-1-piperazineethanesulfonic acid (HEPES), pH 7, and maintained at 37 °C with 5% $CO_2$. Inhibition of liver stage infection was determined by measuring the luminescence intensity in Huh-7 cells infected with a firefly luciferase-expressing *P. berghei* line, *Pb*GFP-$Luc_{con}$, as previously described.[47] Briefly, cells ($12 \times 10^3$/well) were seeded in 96-well plates the day before drug treatment and infection. Tested compounds were prepared in the following way: 10 mM stock solutions were obtained by dissolving accurately weighed compounds in MeOH and dilutions subsequently made with medium to the desired concentration. Medium was replaced by fresh medium containing the appropriate concentration of each compound 1 h prior to infection. Sporozoites (10 000 spz/well), freshly obtained through disruption of salivary glands of infected female *Anopheles stephensi* mosquitos, were added to the wells 1 h after compound addition. Sporozoite addition was followed by centrifugation at 1700*g* for 5 min. At 24 h after infection, the medium was once more replaced by fresh medium containing the appropriate concentration of each compound. Inhibition of parasite development in the liver was measured 48 h after infection. The effect of the compounds on the viability of Huh-7 cells was assessed by the AlamarBlue assay (Invitrogen, U.K.), using the manufacturer's protocol. Nonlinear regression analysis was used to fit the normalized results of the dose−response curves, and $IC_{50}$ values were determined using the SigmaPlot software.

**Rat Microsomes Stability Assay.** The viability of the rat microsomes was initially accessed by evaluating their CYP2E1-catalyzed *p*-nitrophenol hydroxylation capacity, applying a methodology described elsewhere.[49] Two parallel determinations in rat microsomes, with and without NADPH regenerating system, were performed for selected compounds. Compounds were incubated at 37 °C at 1 μM in rat or mouse pooled liver microsomes (0.2 mg of protein/mL, BD Gentest, Discovery Labware Inc., Woburn, MA), suspended in 10 mM phosphate buffer solution (pH 7.4 at 25 °C). Metabolic reactions were initiated by the addition of a NADPH regenerating system A (31 mM $NADP^+$, 66 mM glucose 6-phosphate, and 0.67 mM $MgCl_2$) and NADPH regenerating system B (BD Gentest, containing 40 U/mL glucose 6-phosphate dehydrogenase in 5 mM sodium citrate). At appropriate intervals, aliquots were removed and added to acetonitrile. The samples were mixed and centrifuged for 10 min at room temperature (Σ, 112*g*−4000*g*), and the supernatant fraction was analyzed by HPLC. Measurements were carried out in a LabChrom chromatograph coupled to a Merck Hitachi L-7100 pump, a Shimadzu SPD-5AV UV/vis spectrophotometric detector, and a Merck Hitachi 2500 integrator. A LichroCARTRP-18 (5 μm, 250−254 mm) analytical column (Merck) was used with an acetonitrile/$H_2O$ (25:75, v/v) eluent system. Elution was performed at a solvent flow rate of 1 mL/min. In the assay without NADPH generating system, 24 μL of purified water was used instead of solutions A and B.

## ■ ASSOCIATED CONTENT

### Ⓢ Supporting Information

General procedure for 6- and 7-substituted quinolin-4-amines, structural data of intermediates **7a−j**, X-ray analysis of compound **5c**, NMR spectra of compound **5o**, HPLC conditions and retention times of final compounds **5a−v**, and LC−MS analysis of microsomal incubation mixtures of compound **5u**. This material is available free of charge via the Internet at http://pubs.acs.org.

## ■ AUTHOR INFORMATION


### Corresponding Author

*Phone: +351 217946400. E-mail: aressurreicao@ff.ul.pt.

### Author Contributions

[∞]A.S.R. and D.G. contributed equally.


### Notes

The authors declare no competing financial interest.

## ■ ACKNOWLEDGMENTS


This work was supported by Fundação para a Ciência e Tecnologia (FCT), Portugal, through Grants Pest-OE/SAL/UI4013/2011 and PTDC/SAU-FCF/098734/2008. A.R.S., A.S.R. and M.P. acknowledge FCT for a Ph.D. fellowship (Grant BD/51459/2011), postdoctoral fellowship (Grant BPD/64859/2009), and Programa Ciência 2007, respectively. M.M.M. is a Howard Hughes Medical Institute International Scholar, and P.J.R. is a Distinguished Clinical Scientist of the Doris Duke Charitable Foundation. Purified pHHyDHOD-GFP plasmid was generously provided by Akhil Vaidya (Drexel University College of Medicine, Philadelphia, PA). We also thank the staff and patients of Ward 7Y and the Gastroenterology Unit, Royal Liverpool Hospital, U.K., for their generous donation of blood.


## ■ ABBREVIATIONS USED

CQ, chloroquine; PQ, primaquine; DV, digestive vacuole; NMR, nuclear magnetic resonance; TEA, triethylamine; DEA, diethylamine; rt, room temperature; o/n, overnight; DMF, *N*,*N*-dimethylformamide; THF, tetrahydrofuran; DCM, dichloromethane; DMSO, dimethylsulfoxide; mtETC, mitochondrial electron transport chain; DHODH, dihydroorotate dehydrogenase; HPLC, high performance liquid chromatog-

raphy; LC−MS, liquid chromatography coupled to mass spectrometry

## REFERENCES


(1) *World Malaria Report 2012*; World Health Organization: Geneva, 2012; http://www.who.int/malaria/publications/world_malaria_report_2012/wmr2012_full_report.pdf.

(2) Murray, C. J. L.; Rosenfeld, L. C.; Lim, S. S.; Andrews, K. G.; Foreman, K. J.; Haring, D.; Fullman, N.; Naghavi, M.; Lozano, R.; Lopez, A. D. Global malaria mortality between 1980 and 2010: a systematic analysis. *Lancet* **2012**, *379*, 413−431.

(3) Rodrigues, T.; Moreira, R.; Lopes, F. NEW hope in the fight against malaria? *Future Med. Chem.* **2011**, *3*, 1−3.

(4) Burrows, J. N.; Leroy, D.; Lotharius, J.; Waterson, D. Challenges in antimalarial drug discovery. *Future Med. Chem.* **2011**, *3*, 1401−1412.

(5) Gamo, F. J.; Sanz, L. M.; Vidal, J.; de Cozar, C.; Alvarez, E.; Lavandera, J. L.; Vanderwall, D. E.; Green, D. V. S.; Kumar, V.; Hasan, S.; Brown, J. R.; Peishoff, C. E.; Cardon, L. R.; Garcia-Bustos, J. F. Thousands of chemical starting points for antimalarial lead identification. *Nature* **2010**, *465*, 305−310.

(6) Guiguemde, W. A.; Shelat, A. A.; Bouck, D.; Duffy, S.; Crowther, G. J.; Davis, P. H.; Smithson, D. C.; Connelly, M.; Clark, J.; Zhu, F. Y.; Jimenez-Diaz, M. B.; Martinez, M. S.; Wilson, E. B.; Tripathi, A. K.; Gut, J.; Sharlow, E. R.; Bathurst, I.; El Mazouni, F.; Fowble, J. W.; Forquer, I.; McGinley, P. L.; Castro, S.; Angulo-Barturen, I.; Ferrer, S.; Rosenthal, P. J.; DeRisi, J. L.; Sullivan, D. J.; Lazo, J. S.; Roos, D. S.; Riscoe, M. K.; Phillips, M. A.; Rathod, P. K.; Van Voorhis, W. C.; Avery, V. M.; Guy, R. K. Chemical genetics of *Plasmodium falciparum*. *Nature* **2010**, *465*, 311−315.

(7) Alonso, P. L.; Brown, G.; Arevalo-Herrera, M.; Binka, F.; Chitnis, C.; Collins, F.; Doumbo, O. K.; Greenwood, B.; Hall, B. F.; Levine, M. M.; Mendis, K.; Newman, R. D.; Plowe, C. V.; Rodriguez, M. H.; Sinden, R.; Slutsker, L.; Tanner, M. A research agenda to underpin malaria eradication. *PLoS Med.* **2011**, *8*, e1000406.

(8) Alonso, P. L.; Djimde, A.; Kremsner, P.; Magill, A.; Milman, J.; Najera, J.; Plowe, C. V.; Rabinovich, R.; Wells, T.; Yeung, S. A research agenda for malaria eradication: drugs. *PLoS Med.* **2011**, *8*, e1000402.

(9) Prudencio, M.; Mota, M. M.; Mendes, A. M. A toolbox to study liver stage malaria. *Trends Parasitol.* **2011**, *27*, 565−574.

(10) Wells, T. N. C.; Burrows, J. N.; Baird, J. K. Targeting the hypnozoite reservoir of *Plasmodium vivax*: the hidden obstacle to malaria elimination. *Trends Parasitol.* **2010**, *26*, 145−151.

(11) Mazier, D.; Renia, L.; Snounou, G. A pre-emptive strike against malaria's stealthy hepatic forms. *Nat. Rev. Drug Discovery* **2009**, *8*, 854−864.

(12) Derbyshire, E. R.; Mota, M. M.; Clardy, J. The next opportunity in anti-malaria drug discovery: the liver stage. *PLoS Pathog.* **2011**, *7*, e1002178.

(13) Vale, N.; Moreira, R.; Gomes, P. Primaquine revisited six decades after its discovery. *Eur. J. Med. Chem.* **2009**, *44*, 937−953.

(14) Rodrigues, T.; Prudêncio, M.; Moreira, R.; Mota, M. M.; Lopes, F. Targeting the liver stage of malaria parasites: a yet unmet goal. *J. Med. Chem.* **2012**, *55*, 995−1012.

(15) Meister, S.; Plouffe, D. M.; Kuhen, K. L.; Bonamy, G. M. C.; Wu, T.; Barnes, S. W.; Bopp, S. E.; Borboa, R.; Bright, A. T.; Che, J. W.; Cohen, S.; Dharia, N. V.; Gagaring, K.; Gettayacamin, M.; Gordon, P.; Groessl, T.; Kato, N.; Lee, M. C. S.; McNamara, C. W.; Fidock, D. A.; Nagle, A.; Nam, T. G.; Richmond, W.; Roland, J.; Rottmann, M.; Zhou, B.; Froissard, P.; Glynne, R. J.; Mazier, D.; Sattabongkot, J.; Schultz, P. G.; Tuntland, T.; Walker, J. R.; Zhou, Y. Y.; Chatterjee, A.; Diagana, T. T.; Winzeler, E. A. Imaging of *Plasmodium* liver stages to drive next-generation antimalarial drug discovery. *Science* **2011**, *334*, 1372−1377.

(16) da Cruz, F. P.; Martin, C.; Buchholz, K.; Lafuente-Monasterio, M. J.; Rodrigues, T.; Sonnichsen, B.; Moreira, R.; Gamo, F. J.; Marti, M.; Mota, M. M.; Hannus, M.; Prudêncio, M. Drug screen targeted at *Plasmodium* liver stages identifies a potent multistage antimalarial drug. *J. Infect. Dis.* **2012**, *205*, 1278−1286.

(17) Derbyshire, E. R.; Prudêncio, M.; Mota, M. M.; Clardy, J. Liver-stage malaria parasites vulnerable to diverse chemical scaffolds. *Proc. Natl. Acad. Sci. U.S.A.* **2012**, *109*, 8511−8516.

(18) Lopes, F.; Capela, R.; Goncaves, J. O.; Horton, P. N.; Hursthouse, M. B.; Iley, J.; Casimiro, C. M.; Bom, J.; Moreira, R. Amidomethylation of amodiaquine: antimalarial N-Mannich base derivatives. *Tetrahedron Lett.* **2004**, *45*, 7663−7666.

(19) Lopes, F.; Moreira, R.; Iley, J. Acyloxymethyl as a drug protecting group. Part 6: *N*-Acyloxymethyl- and *N*-(aminocarbonyloxy)methyl sulfonamides as prodrugs of agents containing a secondary sulfonamide group. *Bioorg. Med. Chem.* **2000**, *8*, 707−716.

(20) Iley, J.; Barroso, H.; Moreira, R.; Lopes, F.; Calheiros, T. Acyloxymethyl as a drug protecting group. Part 7: Tertiary sulfonamidomethyl ester prodrugs of benzylpenicillin: chemical hydrolysis and anti-bacterial activity. *Bioorg. Med. Chem.* **2000**, *8*, 1629−1636.

(21) Rodrigues, T.; Moreira, R.; Guedes, R. C.; Iley, J.; Lopes, F. Unanticipated acyloxymethylation of sumatriptan indole nitrogen atom and its implications in prodrug design. *Arch. Pharm.* **2008**, *341*, 344−350.

(22) Iley, J.; Lopes, F.; Moreira, R. Kinetics and mechanism of hydrolysis of *N*-amidomethylsulfonamides. *J. Chem. Soc., Perkin Trans. 2* **2001**, 749−753.

(23) Lim, H. K.; Chen, J.; Sensenhauser, C.; Cook, K.; Preston, R.; Thomas, T.; Shook, B.; Jackson, P. F.; Rassnick, S.; Rhodes, K.; Gopaul, V.; Salter, R.; Silva, J.; Evans, D. C. Overcoming the genotoxicity of a pyrrolidine substituted arylindenopyrimidine as a potent dual adenosine A(2A)/A(1) antagonist by minimizing bioactivation to an iminium ion reactive intermediate. *Chem. Res. Toxicol.* **2011**, *24*, 1012−1030.

(24) Rodrigues, T.; da Cruz, F. P.; Lafuente-Monasterio, M. J.; Goncalves, D.; Ressurreição, A. S.; Sitoe, A. R.; Bronze, M. R.; Gut, J.; Schneider, G.; Mota, M. M.; Rosenthal, P. J.; Prudêncio, M.; Gamo, F. J.; Lopes, F.; Moreira, R. Quinolin-4(1*H*)-imines are potent antiplasmodial drugs targeting the liver stage of malaria. *J. Med. Chem.* **2013**, *56*, 4811−4815.

(25) Rodrigues, T.; Moreira, R.; Dacunha-Marinho, B.; Lopes, F. Bis{(*E*)-3-(diethylmethylammonio)methyl-*N*-3-(*N*,*N*-dimethylsulfamoyl)-1-methylpyridin-4-ylidene-4-methoxyanilinium}tetraiodide pentahydrate. *Acta Crystallogr., Sect. E: Struct Rep. Online* **2009**, *65*, o283−o284.

(26) De, D. Y.; Byers, L. D.; Krogstad, D. J. Antimalarials: synthesis of 4-aminoquinolines that circumvent drug resistance in malaria parasites. *J. Heterocycl. Chem.* **1997**, *34*, 315−320.

(27) Madrid, P. B.; Sherrill, J.; Liou, A. P.; Weisman, J. L.; DeRisi, J. L.; Guy, R. K. Synthesis of ring-substituted 4-aminoquinolines and evaluation of their antimalarial activities. *Bioorg. Med. Chem. Lett.* **2005**, *15*, 1015−1018.

(28) Hansch, C.; Leo, A.; Taft, R. W. A survey of Hammett substituent constants and resonance and field parameters. *Chem. Rev.* **1991**, *91*, 165−195.

(29) Perrin, D. D.; Dempsey, B.; Serjeant, E. P. *pKa Prediction for Organic Acids and Bases*; Chapman and Hall: London, 1981; p 146.

(30) Warhurst, D. C.; Craig, J. C.; Adagu, P. S.; Guy, R. K.; Madrid, P. B.; Fivelman, Q. L. Activity of piperaquine and other 4-aminoquinoline antiplasmodial drugs against chloroquine-sensitive and resistant blood-stages of *Plasmodium falciparum*: role of beta-haematin inhibition and drug concentration in vacuolar water- and lipid-phases. *Biochem. Pharmacol.* **2007**, *73*, 1910−1926.

(31) Egan, T. J.; Combrinck, J. M.; Egan, J.; Hearne, G. R.; Marques, H. M.; Ntenteni, S.; Sewell, B. T.; Smith, P. J.; Taylor, D.; van Schalkwyk, D. A.; Walden, J. C. Fate of haem iron in the malaria parasite *Plasmodium falciparum*. *Biochem. J.* **2002**, *365*, 343−347.

(32) Tilley, L.; Dixon, M. W. A.; Kirk, K. The *Plasmodium falciparum*-infected red blood cell. *Int. J. Biochem. Cell Biol.* **2011**, *43*, 839−842.

(33) Weissbuch, I.; Leiserowitz, L. Interplay between malaria, crystalline hemozoin formation, and antimalarial drug action and design. *Chem. Rev.* **2008**, *108*, 4899−4914.

(34) Combrinck, J. M.; Mabotha, T. E.; Ncokazi, K. K.; Ambele, M. A.; Taylor, D.; Smith, P. J.; Hoppe, H. C.; Egan, T. J. Insights into the role of heme in the mechanism of action of antimalarials. *ACS Chem. Biol.* **2013**, *8*, 133−137.
(35) Hilal, S. H.; Karickhoff, S. W.; Carreira, L. A. A rigorous test for SPARC's chemical reactivity models: estimation of more than 4300 ionization p*K*(a)s. *Quant. Struct.−Act. Relat.* **1995**, *14*, 348−355.
(36) Thomas, V.; Gois, A.; Ritts, B.; Burke, P.; Hanscheid, T.; McDonnell, G. A novel way to grow hemozoin-like crystals in vitro and its use to screen for hemozoin inhibiting antimalarial compounds. *PLoS One* **2012**, *7*, e41006.
(37) Kesten, S. J.; Degnan, M. J.; Hung, J. L.; McNamara, D. J.; Ortwine, D. F.; Uhlendorf, S. E.; Werbel, L. M. Antimalarial drugs. 64. Synthesis and antimalarial properties of 1-imino derivatives of 7-chloro-3-substituted-3,4-dihydro-1,9(2*H*,10*H*)-acridinediones and related structures. *J. Med. Chem.* **1992**, *35*, 3429−3447.
(38) Berman, J.; Brown, L.; Miller, R.; Andersen, S. L.; McGreevy, P.; Schuster, B. G.; Ellis, W.; Ager, A.; Rossan, R. Antimalarial activity of WR 243251, a dihydroacridinedione. *Antimicrob. Agents Chemother.* **1994**, *38*, 1753−1756.
(39) Suswam, E.; Kyle, D.; Lang-Unnasch, N. *Plasmodium falciparum*: the effects of atovaquone resistance on respiration. *Exp. Parasitol.* **2001**, *98*, 180−187.
(40) Rodrigues, T.; Lopes, F.; Moreira, R. Inhibitors of the mitochondrial electron transport chain and de novo pyrimidine biosynthesis as antimalarials: the present status. *Curr. Med. Chem.* **2010**, *17*, 929−956.
(41) Biagini, G. A.; Fisher, N.; Berry, N.; Stocks, P. A.; Meunier, B.; Williams, D. P.; Bonar-Law, R.; Bray, P. G.; Owen, A.; O'Neill, P. M.; Ward, S. A. Acridinediones: selective and potent inhibitors of the malaria parasite mitochondrial bc(1) complex. *Mol. Pharmacol.* **2008**, *73*, 1347−1355.
(42) Cowley, R.; Leung, S.; Fisher, N.; Al-Helal, M.; Berry, N. G.; Lawrenson, A. S.; Sharma, R.; Shone, A. E.; Ward, S. A.; Biagini, G. A.; O'Neill, P. M. The development of quinolone esters as novel antimalarial agents targeting the *Plasmodium falciparum* bc(1) protein complex. *MedChemComm.* **2012**, *3*, 39−44.
(43) Zhang, Y. Q.; Clark, J. A.; Connelly, M. C.; Zhu, F. Y.; Min, J. K.; Guiguemde, W. A.; Pradhan, A.; Iyer, L.; Furimsky, A.; Gow, J.; Parman, T.; El Mazouni, F.; Phillips, M. A.; Kyle, D. E.; Mirsalis, J.; Guy, R. K. Lead optimization of 3-carboxyl-4(1*H*)-quinolones to deliver orally bioavailable antimalarials. *J. Med. Chem.* **2012**, *55*, 4205−4219.
(44) Yeates, C. L.; Batchelor, J. F.; Capon, E. C.; Cheesman, N. J.; Fry, M.; Hudson, A. T.; Pudney, M.; Trimming, H.; Woolven, J.; Bueno, J. M.; Chicharro, J.; Fernandez, E.; Fiandor, J. M.; Gargallo-Viola, D.; de las Heras, F. G.; Herreros, E.; Leon, M. L. Synthesis and structure−activity relationships of 4-pyridones as potential antimalarials. *J. Med. Chem.* **2008**, *51*, 2845−2852.
(45) Biagini, G. A.; Fisher, N.; Shone, A. E.; Mubaraki, M. A.; Srivastava, A.; Hill, A.; Antoine, T.; Warman, A. J.; Davies, J.; Pidathala, C.; Amewu, R. K.; Leung, S. C.; Sharma, R.; Gibbons, P.; Hong, D. W.; Pacorel, B.; Lawrenson, A. S.; Charoensutthivarakul, S.; Taylor, L.; Berger, O.; Mbekeani, A.; Stocks, P. A.; Nixon, G. L.; Chadwick, J.; Hemingway, J.; Delves, M. J.; Sinden, R. E.; Zeeman, A. M.; Kocken, C. H. M.; Berry, N. G.; O'Neill, P. M.; Ward, S. A. Generation of quinolone antimalarials targeting the *Plasmodium falciparum* mitochondrial respiratory chain for the treatment and prophylaxis of malaria. *Proc. Natl. Acad. Sci. U.S.A.* **2012**, *109*, 8298−8303.
(46) Painter, H. J.; Morrisey, J. M.; Mather, M. W.; Vaidya, A. B. Specific role of mitochondrial electron transport in blood-stage *Plasmodium falciparum*. *Nature* **2007**, *446*, 88−91.
(47) Ploemen, I. H. J.; Prudêncio, M.; Douradinha, B. G.; Ramesar, J.; Fonager, J.; van Gemert, G.-J.; Luty, A. J. F.; Hermsen, C. C.; Sauerwein, R. W.; Baptista, F. G.; Mota, M. M.; Waters, A. P.; Que, I.; Lowik, C. W. G. M.; Khan, S. M.; Janse, C. J.; Franke-Fayard, B. M. D. Visualisation and quantitative analysis of the rodent malaria liver stage by real time imaging. *PLoS One* **2009**, *4*, e7881.
(48) Vallieres, C.; Fisher, N.; Antoine, T.; Al-Helal, M.; Stocks, P.; Berry, N. G.; Lawrenson, A. S.; Ward, S. A.; O'Neill, P. M.; Biagini, G. A.; Meunier, B. HDQ, a potent inhibitor of *Plasmodium falciparum* proliferation, binds to the quinone reduction site of the cytochrome bc(1) complex. *Antimicrob. Agents Chemother.* **2012**, *56*, 3739−3747.
(49) Chang, T. K. H.; Crespi, C. L.; Waxman, D. J. Spectrophotometric analysis of human CYP2E1-catalyzed *p*-nitrophenol hydroxylation. *Methods Mol. Biol.* **2006**, *320*, 127−131.